REVIEW

Check for updates

Graphene quantum dots for energy storage and conversion: from fabrication to applications

Qianwen Liu,† Jianhan Sun,† Kun Gao, Nan Chen, [ID] * Xiaotong Sun, Dan Ti, Congcong Bai, Ranran Cui and Liangti Qu [ID] *

As a new kind of zero-dimensional (0D) material, graphene quantum dots (GQDs) have broad prospects in energy storage and conversion due to their unique physical and chemical properties. In addition to the excellent properties of graphene, GQDs also have quantum confinement effects and edge effects. The size of GQDs and types of their edges determine their excellent properties. In this paper, the progress in the synthesis, doping and modification methods of GQDs in recent years is reviewed, and the significant advances of GQDs in energy conversion devices such as supercapacitors/microsupercapacitors, solar cells, batteries and LEDs are summarized. In addition, we rationally analysed the shortcomings of GQDs for energy storage and conversion, and predicted the future development trend of GQD research and its challenges and opportunities.

1 Introduction

Graphene is a two-dimensional (2D) honeycomb monatomic carbon molecular layer with large surface area, intrinsic carrier mobility (15 000 cm^2 V^{-1} s) and excellent mechanical strength and ductility. However, the zero band gap and metal conductivity of graphene severely limited the application of 2D graphene layers in functional materials and devices.[1,2] Fortunately, the emergence and successful preparation of GQDs in time fundamentally overcame these disadvantages. As a 0D carbon-based nanomaterial, GQDs not only exhibit the excellent properties of graphene, but their typical quantum confinement and edge effects benefit from their lateral dimension of less than 10 nm and thickness of less than 2 nm,[3–5] which endows GQDs with broad application prospects in the field of nanomaterials and -devices. For example, GQDs can be used to prepare photo-electric detectors and light emitting diode devices owing to their strong size optical dependence.[4] In addition, through the multiple hot carrier collection mechanism, the introduction of GQDs in silicon-based solar cells could effectively break through the Shockley–Queisser efficiency limit.[5] Furthermore, GQDs inherit the good biocompatibility, excellent chemical inertness and non-toxicity properties of graphene.[5–8] Besides this, GQDs also have a larger specific surface area and better surface grafting than graphene through π–π conjugate bonding.[9] In particular,

Key Laboratory of Photoelectronic/Electrophotonic Conversion Materials, Key Laboratory of Cluster Science, Ministry of Education of China, School of Chemistry and Chemical Engineering, Beijing Institute of Technology, Beijing 100081, P. R. China. E-mail: gabechain@bit.edu.cn, lqu@bit.edu.cn
† Qianwen Liu and Jianhan Sun contributed equally to this work.

Miss Qianwen Liu is currently a master's candidate under the supervision of Prof. Nan Chen and Liangti Qu at the School of Chemistry and Chemical Engineering in the Beijing Institute of Technology (China). Her current research mainly focuses on carbon-based materials and applications in micro-devices in energy conversion/storage.

Qianwen Liu

Mr Jianhan Sun received his bachelor's degree from Lanzhou University in 2018. He is currently a master's candidate under the supervision of Prof. Liangti Qu at the School of Chemistry and Chemical Engineering in the Beijing Institute of Technology (China). His research mainly focuses on carbon-based microporous materials.

Jianhan Sun

a multitude of functional groups in GQDs make them a good non-zero band gap and photoluminescent semiconductor material. Density functional theory found that the band gap of GQDs containing individual aromatic rings reaches about 7.4 eV.[10] Consequently, the original GQDs can be added as a conductive agent to the electrode in energy storage devices such as supercapacitors due to their good conductivity, large specific surface area and ease of doping and modification. It has been reported that top-down and bottom-up approaches are the main methods of manufacturing GQDs.[5] Within these approaches, various techniques for fabricating GQDs with various chemical, size, and luminescent properties have been reported.[11] The modification of GQDs plays an important role in the manufacture of materials and devices, which prompts researchers to make great efforts in the exploration of the chemical functions or reactivity of materials. Compared with the luminescence properties of other semiconductor quantum dots (QDs), as the excitation wavelength increases, the luminescence peak of GQDs broadens and red-shifts, exhibiting fluorescence characteristics associated with the excitation wavelength.[12,13] The prominent luminescent properties of GQDs stimulate their development in biological applications such as bioimaging, biosensors, and cell isolation techniques.[14] Additionally, chemical groups and dopants endow GQDs with intrinsic catalytic properties through band gap alignment, synergistic cooperation, light adsorption enhancement or promotion of charge transfer.[15] Meanwhile, the stability of catalysts is significantly improved owing to the chemical inertness of GQDs. To date, many review articles on the biomedical,[16,17] photocatalytic,[18,19] and environmental[20] applications of GQDs have been published. However, the development of GQDs in energy conversion has rarely been reported.[21] Hence, we introduce the synthesis of universal GQDs, performance tuning, and unique applications in the field of energy conversion and storage. We are committed to providing a comparative and balanced perspective and an in-depth understanding of why GQDs deliver superior applications in energy conversion and storage, including electronics, solar photovoltaic cells, and nanogenerators. We anticipate that this review article will benefit all interested researchers, especially those who are engaged in research utilizing GQDs. Finally, future challenges and possibilities in the field of GQDs are also identified and discussed.

2 Fabrication of GQDs

Considering that GQDs are tiny graphite planes with 0D and atomic thickness (usually only 1 or 2 layers and less than 2 nm thick),

Miss Kun Gao received her bachelor's degree from the Nanjing University of Aeronautics and Astronautics in 2017. She is now a master's candidate under the supervision of Prof. Zhipan Zhang at the Department of Chemistry and Chemical Engineering in the Beijing Institute of Technology (China). Her research studies mainly focus on graphene-based energy conversion and storage devices, especially for photocapacitors.

Kun Gao

Dr Nan Chen is currently a professor at the School of Chemistry and Chemical Engineering in the Beijing Institute of Technology (China). He received his bachelor's degree from China Agricultural University and earned his PhD from the Institute of Chemistry, Chinese Academy of Sciences (ICCAS). His research interests lie in the development of new methods and strategies for fabrication of carbon-based functional materials for various applications.

Nan Chen

Miss Xiaotong Sun is currently a master's candidate under the supervision of Prof. Nan Chen and Liangti Qu at the School of Chemistry and Chemical Engineering in the Beijing Institute of Technology (BIT). Her current research focus lies in the synthesis, functionalization and application of carbon-based nanomaterials.

Xiaotong Sun

Miss Dan Ti is currently a master's candidate under the supervision of Prof. Liangti Qu and Prof. Zhipan Zhang at the School of Chemistry and Chemical Engineering in the Beijing Institute of Technology (BIT). Her research mainly focuses on material and mechanistic studies on water-evaporation power generation.

Dan Ti

the fabrication methods have typically been classified as "top-down" and "bottom-up" approaches.

2.1 Top-down methods

The preparation methods of GQDs from top to bottom contained the following several methods, including hydrothermal and solvothermal, electrochemical, stripping, strong acid oxidation, and electron beam irradiation methods.[22,23] Among them, the hydrothermal and solvothermal synthesis of GQDs is one of the most common methods with simple steps and high yields.

As shown in Fig. 1a, a simple method for synthesizing GQDs is to cut carbon materials with bases such as sodium hydroxide (NaOH) and ammonia. Gong *et al.* obtained biocompatible GQDs with up-conversion properties by using graphene oxide as a raw material, dimethylformamide as a solvent and a nitrogen source through a simple solvothermal method.[24] On the other hand, the electrochemical method is beneficial to obtaining superior GQDs by precise control of their size and shape. After that, high quality GQDs prepared by chemical vapour deposition (CVD) combined with the electrochemical method using 3D graphene were reported (Fig. 1b).[25] GQDs have a narrow particle size distribution, a low molecular weight and an average thickness greater than 1.25 nm. Subsequently, many efforts have been devoted to controlling and regulating the size of GQDs. Using multi-walled carbon nanotubes (MWCNTs) as a carbon source,

Pillai *et al.* prepared GQDs *via* electrochemical oxidation by using a solution of $LiClO_4$ dissolved propylene carbonate as an electrolyte (Fig. 1c).[26] The size of GQDs can be adjusted by controlling the conditions of the electrolysis reaction, such as the temperature and time. Acid oxidation is a method of destroying carbon–carbon bonds and decomposing graphene sheets into small-sized GQDs of less than 100 nm by strong oxidation with a strong acid such as concentrated sulfuric acid, concentrated nitric acid or a mixed acid composed of concentrated sulfuric acid and concentrated nitric acid. The acid oxidation method requires very simple and inexpensive raw materials, which provides a new strategy for the preparation of GQDs. For instance, Ajayan *et al.* synthesized bitumen carbon fiber-based micrometer-GQDs through chemical oxidation and cleavage, and the results show that most of the GQDs obtained have zigzag edge structures with semiconductor characteristics, and their particle size distribution ranges between 1 nm and 4 nm (Fig. 1d).[14] Furthermore, in 2019, Tour *et al.* reported a general method for preparing GQDs by placing various coal sources in sulfuric and nitric acid and sonicating and heating them (Fig. 1e).[27] The GQDs obtained by the improved synthesis method have high crystallinity and good solubility in both water and organic solvents. In 2016, Zhang *et al.* prepared GQDs with a grain diameter of 4–10 nm by using an ultrasonic-assisted chemical stripping method and using O_3 and H_2O_2 to conduct oxidation cutting of GO.[28]

Recently, various synthesis methods of GQDs have been reported. However, several limitations such as complicated synthesis procedures, low production yields, expensive equipment, extreme conditions and high cost have hampered their industrial application progress. The Pei group developed a method of ultrasonic-assisted exfoliation of raw graphitic carbon materials in the liquid-phase for the synthesis of GQDs (Fig. 1f),[29] which enables rapid processing, is environmentally friendly, is low-cost, and can be effectively used for mass production of GQDs in industry. Moreover, the adjustable size and density of GQD defects provide a new strategy for large-scale synthesis of controllable GQDs. Pulsed laser ablation (PLA) is a top-down method with one-step reaction, a short synthesis time, good reproducibility, and a minimal experimental set-up, which has attracted great attention from researchers.[30–32] Thus, the understanding of the

Miss Congcong Bai is currently a master's candidate under the supervision of Prof. Liangti Qu and Dr Yang Zhao at the Beijing Institute of Technology (BIT). Her research mainly focuses on micro-energy storage devices.
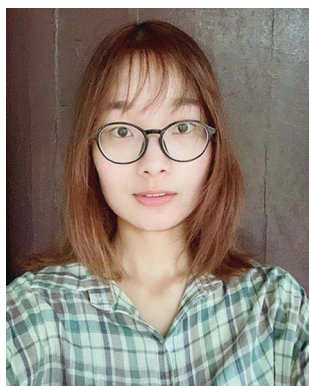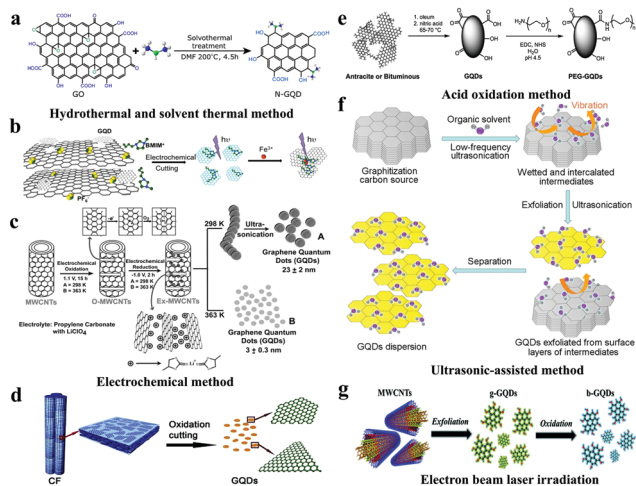
Congcong Bai

Miss Ranran Cui is currently a master's candidate under the supervision of Prof. Zhipan Zhang at the Beijing Institute of Technology (BIT). Her current research focuses on lithium air batteries, especially in the design of battery cathode materials.

Ranran Cui

Prof. Liangti Qu received his PhD in Chemistry from Tsinghua University (China) in 2004. He is now a Professor of Chemistry at the Beijing Institute of Technology (China) and leads the advanced carbon research group. His research interests in materials chemistry mainly focus on the synthesis, functionalization and application of nanomaterials with carbon?carbon conjugated structures, including carbon nanotubes, graphene and conducting polymers.

Liangti Qu

This journal is © The Royal Society of Chemistry and the Chinese Chemical Society 2020

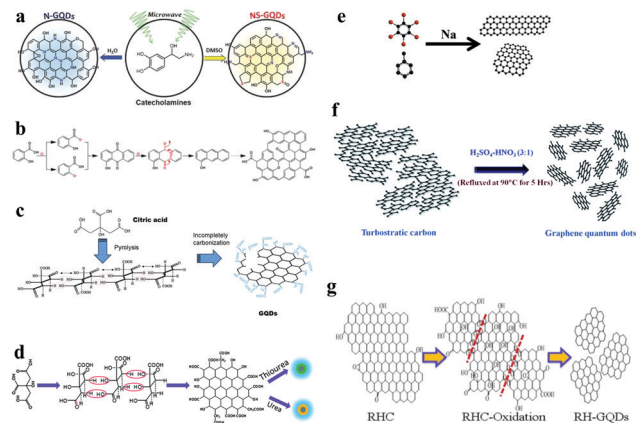*Mater. Chem. Front.*, 2020, **4**, 421–436 | **423**

Fig. 1 Top-down synthesis of GQDs. (a) The solvothermal method to prepare GQDs. (Reproduced with permission from ref. 24, copyright 2013 American Chemical Society.) (b) The electrochemical method to prepare GQDs. (Reproduced with permission from ref. 25, copyright 2014 Wiley-VCH.) (c) The preparation of photoluminescent GQDs from MWCNTs. (Reproduced with permission from ref. 26, copyright 2012 Wiley-VCH.) (d) The oxidation cutting of carbon fibers (CFs) to prepare GQDs. (Reproduced with permission from ref. 14, copyright 2012 American Chemical Society.) (e) The oxidation cutting of coal to prepare GQDs. (Reproduced with permission from ref. 27, copyright 2019 American Chemical Society.) (f) Large-scale synthesis of GQDs by ultrasonic-assisted liquid-phase exfoliation. (Reproduced with permission from ref. 29, copyright 2016 Elsevier B.V.) (g) GQDs synthesized via pulsed laser ablation. (Reproduced with permission from ref. 33, copyright 2016 the Royal Society of Chemistry.)

Fig. 2 Bottom-up synthesis of GQDs. (a) Preparation of N-doped GQDs and N,S-doped GQDs by a microwave-assisted method. (Reproduced with permission from ref. 34, copyright 2016 Wiley-VCH.) (b) Ultraviolet irradiation induces free-radical polymerization to prepare GQDs. (Reproduced with permission from ref. 35, copyright 2017 American Chemical Society.) (c) Preparation of GQDs with citric acid as a monomer. (Reproduced with permission from ref. 36, copyright 2012 Elsevier B.V.) (d) Preparation of N-doped GQDs and N,S-doped GQDs from graphene and urea or thiourea. (Reproduced with permission from ref. 37, copyright 2013 the Royal Society of Chemistry.) (e) Hybrids of GQDs and carbon nanoribbons were synthesized from toluene and hexabromobenzene. (Reproduced with permission from ref. 39, copyright 2015 American Chemical Society.) (f) GQDs cut from graphitized fine carbon powder obtained by deciduous roasting. (Reproduced with permission from ref. 40, copyright 2014 the Royal Society of Chemistry.) (g) GQDs obtained by ultrasonically assisted cutting of graphitized fine carbon powder. (Reproduced with permission from ref. 41, copyright 2016 American Chemical Society.)

photoluminescence (PL) mechanism for GQDs with different wavelengths is expected to be essential for their possible applications in biomedicine, photocatalysis, and optical devices. The Shen group synthesized a series of GQDs with tunable PL by controlling the PLA time.[33] The GQDs implemented using PLA with carboxyl-functionalized MWCNTs exhibit emission colour change from green to blue (Fig. 1g).

2.2 Bottom-up methods

The bottom-up synthesis method refers to constructing from the bottom, that is, the gradual accumulation of atoms, molecules or clusters. The methods for synthesizing GQDs from bottom to up mainly include microwave and ultrasonic methods, solvent chemistry methods, and controlled thermal decomposition of polycyclic aromatic hydrocarbons. Kim et al. obtained nitrogen–sulfur double-doped GQDs by dissolving norepinephrine in DMSO and dialysing the solution after microwave irradiation, which showed good photocatalytic activity. Also, N-doped GQDs can be prepared in the same manner in an aqueous phase system (Fig. 2a).[34] Yang et al. used salicylic acid to prepare GQDs by a free-radical polymerization process. These methods are also suitable for the preparation of heteroatom-doped GQDs, whose by-products are only H_2O and CO_2 (Fig. 2b).[35] Pyrolytic citric acid is also an important monomer for the preparation of GQDs (Fig. 2c).[36] Nitrogen–sulfur double-doped or N-doped GQDs can also be prepared by mixing citric acid with thiourea or urea (Fig. 2d).[37] Nitrogen–sulfur double-doped GQDs have been

synthesized via a one-pot pyrolysis approach using citric acid and L-cysteine as precursors.[38] Wang et al. found that sodium-catalyzed reduction of methylbenzene and hexabromobenzene could produce hybrids of GQDs and carbon nanoribbons (Fig. 2e).[39]

In recent years, synthesis methods combining top-down and bottom-up methods have been studied in depth. For example, a graphitized carbon fine powder is obtained by calcining organic molecules in an inert gas atmosphere, which is a typical bottom-up synthesis concept. The graphitized fine carbon powder is then sheared to form GQDs, which is a typical top-down synthesis concept. After burning neem leaves in an inert gas atmosphere to obtain fine carbon powder, Ogale et al. converted the above carbon powder into GQDs using sulfuric acid and nitric acid. The GQDs prepared in this manner were used as a photoluminescence switch on-off-on probe for Ag^+ ions (Fig. 2f).[40] GQDs can also be prepared by mixing carbon powder with sulfuric acid in ultrasound and then reacting the mixture with nitric acid. At this time, the fine carbon powder in the synthesis method is obtained by baking rice husks (Fig. 2g).[41]

In summary, top-down and bottom-up methods are typical common methods of fabricating GQDs. Consequently, we briefly compared these two methods in terms of the differences in fabrication methods, sizes, quantum yields and applications in recent years. As can be seen in Table 1, the main advantages of the top-down method are the availability of raw materials,

Table 1 Top-down synthesis of GQDs

Product type	Raw material(s)	Subclassification method	Lateral size of GQDs (nm)	Quantum yield (%)	Application(s)
N-GQDs[42]	As-synthesized graphene oxide (GO) sheets	Hydrothermal cutting	5–10	—	Catalytic activity
Amino-N-GQDs[43]	GO sheets	Ultrasonic shearing	7.31 ± 0.50	33	—
GQDs[44]	XC-72 carbon black	Chemical oxidation	4.1 ± 0.8	—	Electrochemilu-minescence biosensors
GQDs[45]	Graphite rods	Electrochemical method	20	18.95	Ion sensors and bioimaging
NP-GQDs[46]	Citric acid and titanium butoxide	Solvothermal treatment	3.03 ± 1.01	8.45	Photocatalytic degradation of dyes
GQDs[47]	Graphite	Acid vapor cutting	3–5	—	Electron transport layers for PSEs
N-O-GQDs[48]	Pyrene	Molecular fusion	2.4–4.8	—	Micro-supercapacitors
N-GQDs[49]	Glucosamine	Microwave-assisted hydrothermal method	6	32	Solar cells

Table 2 Bottom-up synthesis of GQDs

Product type	Raw material(s)	Subclassification method	Lateral size of GQDs (nm)	Quantum yield (%)	Application
NS-GQDs[34]	Norepinephrine	Microwave assisted solvothermal treatment	4.1	17	Photocatalysts
N-GQDs[35]	Norepinephrine	Microwave assisted solvothermal treatment	3.4	7	Photocatalysts
GQDs[36]	Salicylic acid	Stepwise organic synthesis	1–5	81	Fluorescence bioimaging
GQDs[37]	Citric acid	Pyrolysis	15	9.0	Photoluminescence/ photocatalytic
NS-GQDs[39]	Citric acid and L-cysteine	Intermolecular condensation	2.56–3.64	71	Photocatalysts
GQDs[40]	Hexabromobenzene	Stepwise organic synthesis	5	—	Oxygen reduction reaction
GQDs[41]	Dead neem leaves	Carbonization of organic precursors	5–6	1% taking quinine sulphate as a reference	Photoluminescence switch on-off-on probe for Ag^{+} ions

low price, and simple technological processes, with a high quantum yield, which can be used for large-scale production. The commonly used raw materials are mainly large molecular substances such as graphite. However, it is noticed that the size of GQDs is not adjustable based on top-down methods. Among the several top-down methods, the hydrothermal and solvothermal synthesis methods are relatively widely used, while the sizes of GQDs prepared by the molecular fusion method and the acid vapor cutting strategy are relatively small.

The bottom-up method is the second largest technique for preparing GQDs. In Table 2, it is worth noting that this method requires that appropriate carbon-containing precursors be selected, such as aromatic structural molecules, and the operation process is complex. Moreover, some carbon precursors are also difficult to obtain, which presents some obstacles to the preparation of GQDs. Furthermore, the quantum yield of GQDs is relatively low in most bottom-up synthesis methods. Since each coin has two sides, the advantage of the bottom-up method is that the precision of the product can be accurately controlled.

3 Modification of GQDs

3.1 Heteroatom doping

Heteroatom doping has become an effective method for modulating the properties of nanomaterials. N-type or P-type doping can effectively change the electronic structure in a semiconductor material. For example, the electron density of graphene layers can be altered by doping the electron donor and acceptor structures.

Doped GQDs are an example of doped semiconductor materials, in which the main element C in GQDs is partially replaced with some miscellaneous elements such as N, S, Se, B, P, I and Si.[24,50,51] This substitution will change the properties of GQDs; for example, the doping with S and Se will increase the visible absorption of GQDs.[52] The introduction of heteroatoms, a common modification method, has been shown to greatly improve even some of the physical and chemical properties of innovative GQDs. Most non-metallic heteroatoms including N, B and other elements in the structural spatial grid of graphene effectively replace carbon atoms and form electron cloud migration to generate electron holes, which will help doped GQDs play a great role in fuel cells, catalysts and electrochemical capacitors. For the chemical doping with heteroatoms, N and C atoms have similar radii and compact electronegativity. The N donor atom plays a crucial role in the electronic modification of graphene, including improving the conductivity, catalysis and fluorescence of graphene. At present, the N doping methods of GQDs mainly include chemical vapor deposition (CVD),[53,54] the thermolysis method[55] and plasma treatment.[56]

In 2012, the Qu group successfully integrated N-doping and quantum effects, and obtained N-doped GQDs (N-GQDs) for the first time.[57] N-GQDs with excellent luminescent properties and high efficiency oxygen reduction catalysis were prepared by introducing the N atom into the central position of acetone triol sing tetrabutylammonium perchlorate as electrolyte. Currently, functional materials are of important scientific and technological significance due to their valuable applications in photodetectors, solar cells, and bioimaging. However, GQDs with NIR emission

This journal is © The Royal Society of Chemistry and the Chinese Chemical Society 2020

Mater. Chem. Front., 2020, **4**, 421–436 | **425**

have not been reported. In 2014, Lau reported a facile one-step synthesis of polyacrylonitrile (PAN)-based CFs to obtain N-doped GQDs.[58] Noteworthily, the N/C and O/C atomic ratios and N bond configurations in the prepared GQDs can be easily adjusted by changing the heat treatment temperature of CFs. As shown in Fig. 3a, monodisperse N-GQDs having different particle sizes can be prepared by the microwave-assisted hydrothermal method (MAH) using glucose and ammonia as starting materials. Due to the hierarchical structure of N-GQDs, a wide π-conjugated system is generated, resulting in an optical response range of 365 to 980 nm for N-GQDs and a response rate of 325 V W^{-1} at 405 nm.

In the periodic table, B and C are adjacent to each other and have similar atomic radii. Compared to the C atom, the B atom has one less electron in its outermost shell. People are very interested in exploring the properties of B-doped GQDs (B-GQDs), because if some C atoms in graphene are replaced with B atoms, some electronic defects will appear in the products which exhibit some unique properties.[59] Metal-free B-GQDs were prepared by introducing vacancies and elemental boron molecules as substitutional defects. For example, Zhang et al. demonstrated in 2017 that defects of GQDs provide several active sites by decomposition of 4-vinylphenylboronic acid (VPBA) and boric acid, thereby triggering the formation of B-GQDs (Fig. 3b).[60] The B-GQDs were synthesized from VPBA using boric acid as a precursor at 200 °C. Additionally, in the presence of boric acid, B-GQDs can be synthesized by a one-step method with simple operation, low temperature and hydrothermal treatment of glucose (Fig. 3c).[61] B-GQDs possess relatively uniform nano-size and a high B-doping level, the content of which is

about 4.25%. In addition to monoatomic doping, many GQDs are modified by diatomic or triatomic doping. Doping atoms can change the energy band gap and surface properties of GQDs, resulting in enhancement of the photoelectric properties and an increase in the quantum yield of GQDs. Assembled N and S co-doped GQDs (NS-GQDs) obtained by microwave treatment of glucosamine show great potential in organic light-emitting devices as optoelectronic devices.[62] In 2015, also by microwave treatment of CNTs in ionic liquids, S, N and F co-doped GQDs (NFS-GQDs) were successfully obtained (Fig. 3d).[63] Further, Pillai et al. modified a TiO$_2$ mesoporous network with NSF-GQDs, which improved the light capture efficiency of the product. As the band gap of TiO$_2$ was reduced by N doping, the PCE value reached 11.7%. In addition, S was used to promote the electron transfer process, and F played an effective role in binding to the surface of TiO$_2$.[64] N or O doping is beneficial to increase the interface wettability of the carbon electrode to the aqueous electrolyte, thereby enhancing the faradaic reaction dynamics.[48] Inspired by this, the Wu group reported the first application of heavily GQDs co-doped with N and O in MSCs, with improved molecular melting methods, where the N and O contents were as high as 17.8 at% and 21.3 at%, respectively (Fig. 3e).[62]

3.2 Functionalization

The functionalization of GQDs will effectively improve the performance of GQDs, especially their optical properties. The main mechanism is to improve the electronic properties of graphene by adding electron-accepting groups and electron-donating groups. At the same time, the acidic functionalization of GQDs sometimes endows them with catalytic properties, which can be used as acidic solid catalysts for organic reactions. In oxidized GQDs, the type and amount of oxygen-containing functional groups will affect their properties. Qu et al. found that graphene oxide quantum dots containing carbonyl and carboxyl groups can be used as peroxidase mimics (Fig. 4a).[65] Mohammad-Rezaei et al. oxidized rGO with nitric acid and sulfuric acid under microwave conditions.[66] The carboxyl functionalized GQDs they obtained were used to catalyse the coupling reaction of 2-naphthol with a benzaldehyde derivative (Fig. 4b). Chen et al. obtained sulfonated GQDs by reacting chlorosulfonic acid with GQDs at 70 °C for 24 h under nitrogen protection.[67] The sulfonated GQDs show good biomass catalytic capabilities, such as catalyzing the dehydration of fructose to form 5-HMF (Fig. 4c).

Okamoto et al. synthesized amino-functionalized GQDs by hydrothermally mixing ammonia solution and graphene oxide sheets at 70–150 °C for 5 h,[68] the amino groups of which are mainly located at the edge of the sheet, which facilitates precise control of the optical properties of GQDs (Fig. 4d). Pang et al. produced amino-functionalized GQDs by acid-catalyzed dehydration of 1,2-diamine and graphene oxide sheets (Fig. 4e).[69] Rhee et al. also chemically functionalized GQDs using a variety of aniline derivatives that can be used as light sources to produce high purity red-green and orange LEDs (Fig. 4f).[70] A study by Matsui et al. showed that the N-containing groups in N-functionalized GQDs can systematically modify the electronic structure to cause effective orbital resonance of the HOMO and LUMO levels of the GQDs.[71] Further, the
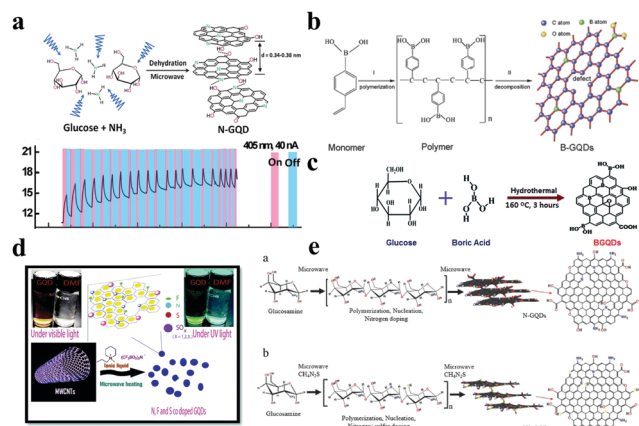

Fig. 3 Heteroatom doping of GQDs. (a) N-GQDs synthesized by a microwave-assisted method and their photoresponses (Φ = 4.0 nm) when irradiated with 405 nm. (Reproduced with permission from ref. 58, copyright 2014 American Chemical Society.) (b) One-pot synthesis procedure for GH-BGQDs using glucose. (Reproduced with permission from ref. 60, copyright 2017 Wiley-VCH.) (c) The synthesis procedure for B-GQDs with glucose. (Reproduced with permission from ref. 61, copyright 2017 the Royal Society of Chemistry.) (d) The formation of co-doped GQDs; the inset shows a comparison of the same concentration of co-doped GQDs in DMF under visible light and UV light respectively. (Reproduced with permission from ref. 63, copyright 2018 the Royal Society of Chemistry.) (e) The growth mechanism of N-GQDs and NS-GQDs with microwaves. (Reproduced with permission from ref. 62, copyright 2015 Wiley-VCH.)

426 | Mater. Chem. Front., 2020, 4, 421–436

This journal is © The Royal Society of Chemistry and the Chinese Chemical Society 2020
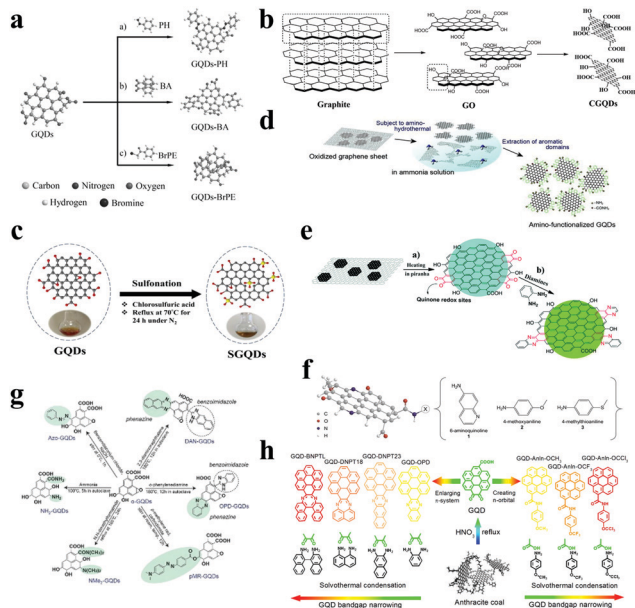
Fig. 4 Functionalization of GQDs. (a) Modification of (a) carbonyl, (b) hydroxy and (c) carboxyl groups on oxidized GQDs. (Reproduced with permission from ref. 65, copyright 2015 Wiley-VCH.) (b) Preparation of carboxylic acid functionalized GQDs. (Reproduced with permission from ref. 66, copyright 2015 the Royal Society of Chemistry.) (c) Preparation of sulfonated GQDs. (Reproduced with permission from ref. 67, copyright 2018 Elsevier B.V.) (d) Preparation of amino-functionalized GQDs. (Reproduced with permission from ref. 68, copyright 2012 Wiley-VCH.) (e) Preparation of amino-functionalized GQDs from graphene oxide sheets. (Reproduced with permission from ref. 69, copyright 2015 the Royal Society of Chemistry.) (f) Synthesis of chemically functionalized GQDs using aniline derivatives and GQDs. (Reproduced with permission from ref. 70, copyright 2016 Nature.) (g) Synthesis of N-functionalized GQDs. (Reproduced with permission from ref. 71, copyright 2016 Wiley-VCH.) (h) Adding a large conjugated functional group to expand the conjugated structure of GQDs. (Reproduced with permission from ref. 72, copyright 2018 American Chemical Society.)

prepared N-functionalized GQDs exerted an excellent effect in the field of perovskite solar cells and phototransistors (Fig. 4g). Chen *et al.* found that the band gap of GQDs can be narrowed by extending the π-conjugated system or functionalizing the electron-donating groups of GQDs,[72] so that the narrow band gap GQDs can be applied to photocatalytic water splitting and high performance CO_2 reduction (Fig. 4h).

4 Applications of GQDs in energy conversion and storage devices
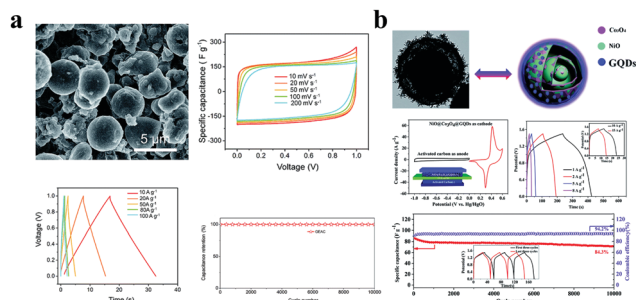
4.1 Supercapacitors/micro-supercapacitors

As energy storage devices, supercapacitors/micro-supercapacitors (SCs/MSCs) are receiving more attention due to their high power density, small size, short charging and discharging processes, and long lifespans. Basically, SCs/MSCs are divided into electrochemical double layer capacitors and pseudocapacitors because of their different charge storage mechanisms. Generally, SCs/MSCs having GQDs as electrode materials belong to an electrochemical double layer type, and its mechanism is charge adsorption on the surface of the electrode. Xue *et al.* electrodeposited GQDs
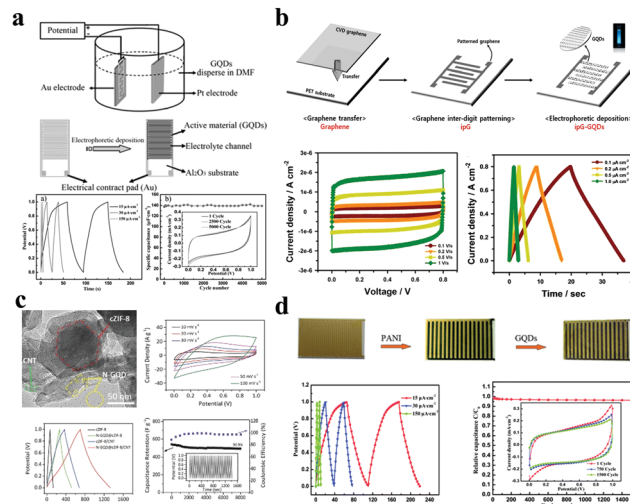
Fig. 5 GQDs as SC/MSC electrodes. (a) GQD interdigitated MSC. (Reproduced with permission from ref. 73, copyright 2013 Wiley-VCH.) (b) Flexible transparent MSC using chelated graphene and GQDs. (Reproduced with permission from ref. 74, copyright 2016 Elsevier B.V.) (c) SC developed with N-GQD@ cZIF-8/CNT electrodes. (Reproduced with permission from ref. 75, copyright 2018 Wiley-VCH.) (d) GQD/PANI asymmetric MSC. (Reproduced with permission from ref. 76, copyright 2013 the Royal Society of Chemistry.)

on a gold finger electrode; the obtained MSC has a specific capacitance of 534.7 μF cm^{-2}, a rate performance of up to 1000 V s^{-1}, and a specific capacitance of 97.8% after 5000 cycles relative to its initial specific capacitance.[73] At the same time, the MSC also has a short relaxation time constant as shown in Fig. 5a (τ_0 = 103.6 μs in aqueous electrolyte and τ_0 = 53.8 μs in ionic liquid electrolyte). Lee *et al.* developed a flexible transparent MSC using chelated graphene and GQDs with a specific capacity of 9.09 μF cm^{-2}, which has a high transmittance of 92.97% at a wavelength of 550 nm and highly bendable characteristics.[74] In the case of the bend, it is still possible to maintain long cycle stability (approximately 100% retention of its initial specific capacitance after 10 000 continuous cycles) (Fig. 5b).

The capacitive mechanism of pseudocapacitors is the reversible faradaic reactions occurring on the electrodes. SCs/MSCs made of carbon quantum dots doped with elements such as N and S are typical pseudocapacitors. Wu *et al.* used carbonized ZIF-8 as a self-sacrificing template, CNTs as a conductive network, and N-doped GQDs as a highly pseudocapacitive material to fabricate SCs. Their SCs have a high specific capacitance of 540 F g^{-1} at 0.5 A g^{-1} in 1 M H_2SO_4 electrolyte and have excellent cycle stability (approximately 90.9% retention of its initial specific capacitance after 8000 continuous cycles). The assembled SC has an energy density of 18.75 W h kg^{-1} and a power density of 108.7 W kg^{-1} (Fig. 5c).[75] Asymmetric SCs/MSCs are also a large class of pseudocapacitors. Among them, GQD/polymer material asymmetric SCs are extremely representative. For example, Xue *et al.* developed a GQD/PANI asymmetric MSC, which has a specific capacity of 667.5 μF cm^{-2}, a rate capability of up to 1000 V s^{-1}, a very short relaxation time (τ_0 = 115.9 μs in aqueous electrolyte), and great cycle stability (67.8% of its initial value after 1500 cycles).[76] Moreover, the energy density of the SC was 0.093 μW h cm^{-2}

Fig. 6 GQDs as supercapacitor additives. (a) GQDs as a conductive agent added to ultra-high specific surface area activated carbon SCs. (Reproduced with permission from ref. 77, copyright 2019 the Royal Society of Chemistry.) (b) GQDs as a conductive agent added to transition metal oxide pseudocapacitive SCs. (Reproduced with permission from ref. 78, copyright 2019 the Royal Society of Chemistry.)

and the power density was as high as 7.52 $\mu W\ cm^{-2}$ (Fig. 5d). In addition, due to their excellent conductivity, GQDs can also be used as an auxiliary in SCs to enhance the properties of the electrode. Fan et al. embedded GQDs into an electrode made of high specific surface area carbon material to improve the conductivity of the electrode.[77] The electrical double layer SC has a specific capacitance of 388 F g^{-1} at 1 A g^{-1} with excellent rate performance ($\tau_0 = 0.68$ s) and cycle stability in a two-electrode system (100% of its initial value after 10 000 cycles). At a high current density of 100 A g^{-1}, the SC has a capacitance retention of 60% (Fig. 6a). Transition metal compounds are a class of materials with high pseudocapacitance, but it is difficult to use them alone as electrodes because of their poor electrical conductivity, structural stability, rate performance, and cycle stability. However, the addition of GQDs will effectively enhance the above performance. Wang et al. synthesized a multi-layer $NiO@Co_3O_4$ hollow sphere decorated with GQDs as the cathode of SCs, and activated carbon as the anode to form asymmetric SCs.[78] The asymmetric SCs have a specific capacitance of 1361 F g^{-1} and an energy density of 38.44 W h kg^{-1} and high cycle stability (76.4% retention after 3000 cycles) (Fig. 6b). In conclusion, Tables 3 and 4 display different properties and performances of GQDs in MSCs (Table 3) and SCs (Table 4).

4.2 Solar cells

Incorporation of GQDs into nanomaterials offered the opportunity for the picturesque charge carrier extraction capability for the enhancement of solar cell efficiency, owing to their unique opto-electronic characteristics, up-conversion field luminescence characteristics and band gap tunability and low application cost. GQDs have broad application prospects in high-performance photo-voltaic devices, such as perovskite solar cells,[85,86] organic and inorganic hybrid solar cells,[87] and dye-sensitized solar cells.[88,89] GQDs have a large specific surface area, high electron mobility and an excellent ability to absorb ultraviolet light and convert it into visible light, and are widely used as a sensitizer, an electron/hole transport layer, or an active layer additive for photovoltaic devices.

4.2.1 Perovskite solar cells. Perovskite solar cells (PSCs) have attracted widespread attention for decades due to their high performance and simple manufacturing processes.[90] Finding suitable additives to add to PSCs to improve their performance is as important as the manufacturing process of highly efficient perovskite films.[91,92] Several advanced nanomaterials, such as GQDs and tiny graphene layers, offer tunable band gaps and good chemical stability. Furthermore, GQDs are excellent electron acceptors and donors during photoexcitation.[93] In 2017, the Jang group reported different-sized GQD modified TiO_2 layers to

Table 3 GQDs applied to MSCs

Electrode material	Electrolyte	Specific capacity ($\mu F\ cm^{-2}$)	Rate performance (V s^{-1})	Energy density ($\mu W\ h\ cm^{-2}$)	Power density ($\mu W\ cm^{-2}$)	Operating voltage (V)	Cycle stability
GQD//GQD[73]	0.5 M Na_2SO_4	534.7	1000	0.074	7.5	1	97.8%, 5000 cycles
GQD//GQD[73]	2 M $EMIMBF_4$/AN	468.1	—	0.474	56.7	2.7	94%, 5000 cycles
GQD//MnO_2[73]	0.5 M Na_2SO_4	1107.4	—	0.154	7.51	1	93.3%, 5000 cycles
N-O-GQD//N-O-GQD[48]	1 M H_2SO_4	5790	—	8.0	75	1	82.6%, 5000 cycles
GQD//MnO_2[79]	0.5 M Na_2SO_4	2980	—	0.414	15.01	1	—
GQD//PANI[76]	0.5 M Na_2SO_4	667.5	1000	0.093	7.52	0.9	97.3%, 1500 cycles

Table 4 GQDs applied to SCs

| Electrode material	Electrolyte	Specific capacity (F g^{-1})	Rate performance (V s^{-1})	Energy density (W h kg^{-2})	Power density (W kg^{-2})	Operating voltage (V)	Cycle stability
N-GQD@cZIF-8/CNT//N-GQD@cZIF-8/CNT[75]	H_2SO_4/PVA	400	1000	14	89.5	1	82%, 5000 cycles
GEAC//GEAC[77]	Alkaline electrolyte	388	—	13.47	12 500	1	100%, 10 000 cycles
$NiO@Co_3O_4@GQD$//AC[78]	KOH/PVA	123	—	38.44	11 251	1.6	84.3%, 10 000 cycles
CoDC-0.5//CoDC-0.5[80]	6 M KOH	240	—	9.38	1250	1	90%, 10 000 cycles
Amine-GQD-TNA//amine-GQD-TNA[81]	1 M H_2SO_4	595	—	21.8	25 000	1	90%, 10 000 cycles
N-GQD@Fe_3O_4-HNT electrode (three-electrode test system)[82]	1 M Na_2SO_4	418	1000	29	5200	1	82%, 3000 cycles
GQD/$NiCo_2S_4$ electrode (three-electrode test system)[83]	3 M KOH	678.22	—	—	—	0.46	92%, 5000 cycles
GQD-3DG//GQD-3DG[84]	1 M H_2SO_4	268	—	—	—	0.8	90%, 5000 cycles

achieve efficient planar perovskite solar cells.[94] As shown in Fig. 7a, GQDs reduce the contact resistance and effective electron transfer at the perovskite/TiO$_2$ interface, which can reduce the series resistance, increase the compound resistance of the device, and improve the open circuit voltage (V_{oc}) and fill factor (FF). The GQDs extend all pv parameters to achieve the best PCE of 19.11%. Several studies have indicated that the development of organic–inorganic halide perovskites is limited due to their poor stability under high temperature and humidity conditions.[95,96] Recently, the Liu group constructed inorganic γ-CsPbI$_3$ perovskite solar cells based on N-GQDs.[97] The N-GQD material is stable to humidity and high temperature stress. In addition, the modified PSC showed a significant increase in short circuit current density (JSC) from 9.15 mA cm^{-2} to 18.67 mA cm^{-2}, and the PCE also increased from 15.53% to 16.02% (Fig. 7b).

It has been reported that significant electron accumulation caused by the charge barrier at the TiO$_2$/perovskite interface

always exists, resulting in increased hysteresis and reduced efficiency.[98,99] Moreover, TiO$_2$ suffers from low electron mobility (*ca.* 10^{-4} cm^2 V^{-1} s^{-1}), and requires sintering at a high temperature (*ca.* 400 °C), which limits the establishment of flexible PSCs.[100,101] Inspired by this, in 2018, the Lin group designed a facile way to prepare GQD and SnO$_2$ nanoparticle composites as electron transport layers (ETLs) for highly efficient rigid and flexible PSCs (Fig. 7c).[102] As is known to all, low temperature SnO$_2$ films can be processed *via* various methods such as spin-coating solution,[103–105] chemical-bath deposition,[106] and atomic layer deposition (ALD).[107] However, several devices based on low-temperature solution suffer from serious hysteresis, making it difficult to determine their real PCEs.[103–105] Consequently, the Yang group exploited high performance and very little hysteresis N–I–P planar PSCs with SnO$_2$:GQDs as ETLs.[108] In Fig. 7d, the Fermi level (E_F) of the SnO$_2$:GQDs decreases from 4.35 to 4.01 eV because the electron concentration increased through illumination. Moreover, the electron mobility of the SnO$_2$:GQDs has improved from 6.72 × 10^{-4} to 1.01 × 10^{-3} cm^2 V^{-1} s after illumination. Conclusively, the planar PSCs based on SnO$_2$:GQDs ETLs achieve a maximum steady-state efficiency of 20.23% with very little hysteresis. This research provides a simple and valid method to increase device efficiency by enhancing the electronic properties of the ETLs. Similarly, organic transport layers such as [6,6]-phenyl C61 butyric acid methyl ester PCBM[109] and PCBDAN[110] have attracted considerable attention due to their simple and low-temperature production process. Unfortunately, the intrinsic low electrical conductivity and electron mobility of PCBM still hinder the promotion of PSCs.[111] In 2017, the Yang group reported a powerful method to enhance planar PSCs' performance by using GQDs as a planar PCBM ETL with additional forward PSCs not only to dramatically increase the PCE of PSCs, but also to increase the light stability of the devices.[112] Their PCE increased from 14.68 to 17.56, while the PCBM:GQD device maintained an original maximum of approximately 80% over a continuous full-spectrum sunshine time of more than 300 h (Fig. 7e). Then, in order to better verify the impact of GQD doping on PCBM performance, the authors used PCBM and PCBM:GQDs as ETLs to obtain sandwich structure devices. The results show that the conductivity is one order of magnitude higher than that of pure PCBM under GQD doping conditions. In summary, the introduction of GQDs into the perovskite thin film not only effectively passivates large chunks of grain boundaries and eliminates electron traps, thereby reducing charge recombination, but also promotes electron transfer in the perovskite layer.

4.2.2 Organic and inorganic hybrid solar cells. Photon down-conversion is one of the GQDs' features of optical applications that helps them absorb photons in shorter wavelength regions as well as emit photons in longer wavelength regions. The He group used GQDs as the down-conversion material of silicon heterojunction solar cells. When the amount of GQDs added is 0.3 wt%, the short-circuit current (JSC) of the solar cells increases from 35.31 mA cm^{-2} to 37.47 mA cm^{-2}.[113] By using GQDs in PEDOT:PSS, Si/PEDOT:PSS hybrid solar cells can achieve an efficiency of 13.22%.[114] Upon introduction of GQDs as the photon down-conversion additive in PEDOT:PSS,
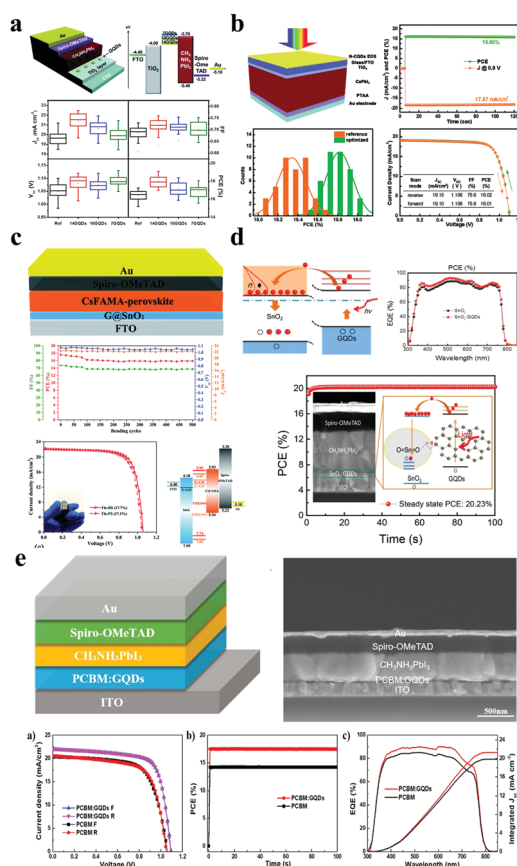
Fig. 7 GQDs for perovskite solar cell devices. (a) GQD modified TiO$_2$ layer for efficient planar perovskite solar cells. (Reproduced with permission from ref. 94, copyright 2013 the Royal Society of Chemistry.) (b) NN-GQDs for inorganic γ-CsPbI$_3$ perovskite solar cells. (Reproduced with permission from ref. 97, copyright 2019 the Royal Society of Chemistry.) (c) GQD/SnO$_2$ composites for flexible perovskite photovoltaics. (Reproduced with permission from ref. 102, copyright 2019 the Royal Society of Chemistry.) (d) The perovskite solar cells with the structure of SnO$_2$:GQD PSCs. (Reprinted with permission from ref. 108, copyright 2017 American Chemical Society.) (e) Perovskite solar cells with a GQD doped PCBM electron transport layer. (Reproduced with permission from ref. 112, copyright 2017 Elsevier B.V.)

This journal is © The Royal Society of Chemistry and the Chinese Chemical Society 2020

Mater. Chem. Front., 2020, **4**, 421–436 | **429**

the hybrid device achieves a high detection rate of 8×10^{11} Jones without any bias voltage applied.[115]

4.3 Li$^+$/Na$^+$ batteries

In Li$^+$ or Na$^+$ batteries, GQDs can effectively alleviate volume expansion,[116] increase the diffusion speeding of Li$^+$/Na$^+$,[117,118] increase electron transfer,[119] and improve electrochemical performance.[120,121] Therefore, when GQDs are used as an anode material or mixed with an active material as an auxiliary agent, the electrochemical performance will be improved.

Due to its advantages of large capacity, low cost, and abundant sources, VO$_x$ is considered to be a promising lithium ion battery electrode material.[122,123] So far, various forms of VO$_2$ nanostructures have been prepared for use as lithium-ion battery (LIB) cathode materials. However, most of these materials show rapid capacity decay and poor high-speed performance, and the resistance tends to increase rapidly during cycling. In 2015, the Fan group first reported the application of GQDs in batteries (VO$_2$@GQD) as an efficient surface "sensitizer" and "stabilizer" to coat the VO$_2$ surface by electrophoresis.[124] It is well known that GQDs can improve electrochemical performance and separate VO$_2$ nanomaterials from each other, thereby avoiding agglomeration and minimizing the dissolution of active substances.[122] As shown in Fig. 8a, after 1500 cycles at 18 A g^{-1}, the GVG electrode has a capacity exceeding 420 mA h g^{-1} and a capacity retention rate of 94%. Moreover, VO$_2$@GQD exhibits a high capacity of 306 mA h g^{-1} and superior rate tolerance and a lower capacity decay (12% after 1500 cycles at 18 A g^{-1}) with a power density of 42 kW kg^{-1} at an energy density of more than 100 W h kg^{-1}. Recently, great efforts have been made towards exploring new applications for high-performance LIBs.[125–127] The existing LIBs have short cycle lives and low power density, which cannot meet the efficient storage requirements of renewable energy and/or electric vehicles or HEVs.[128] Therefore, the current work is to improve the energy density, power density and cycle life of electrode materials. In 2019, the Kim group reported a fresh LTO/N-GQD/super-hierarchical anode material for LIBs.[129] Compared to pure LTO (Li$_4$Ti$_5$O$_{12}$), the LTO with N-GQDs increases the specific capacity by 23% and exhibits better electrical properties, such as discharge capacity maintained at about 170 mA h g^{-1} at 20 °C for over 200 cycles as shown in Fig. 8b. The development and utilization of porous materials have received extensive attention in energy storage and conversion.[130,131] Among them, metal organic frameworks (MOFs) have the advantages of colossal surface area, anisotropic structure, multifunctional pores and high carbon content of organic ligands, which are beneficial for preparing porous materials.[132,133] However, the poor conductivity and instability of porous materials still limit their widespread use in batteries. In order to solve these shortcomings, the Yuan group synthesized porous carbon derived from ZIF-8@GQDs and the electrode material showed excellent electrochemical performance.[134] The electrode material of lithium battery has a long cycle stability on account of that GQDs were loaded onto the surface of the MOF derivative ZIF-8 to form a cathode material of LIBs.

Among the various anode candidates, TiO$_2$ is widely used because of its environmental friendliness, safety, low cost, and good chemical stability.[135,136] It is regrettable that the poor capacity and low rate performance of a TiO$_2$ anode limit its practical application. Thus, increasing the electrochemical performance of the TiO$_2$ anode is the key problem. In 2018, the Wei group successfully designed and fabricated a TiO$_{2-x}$/GQD hybrid.[137] TiO$_2$ embedded with GQDs has higher electronic conductivity and higher specific surface area. Moreover, as displayed in Fig. 8c, the TiO$_{2-x}$/GQD anode exhibited an excellent Li-storage capacity of 168.5 mA h g^{-1} at 5 °C and a long-term cycling performance of 160.1 mA h g^{-1} over 500 cycles at 10 °C.

Recently, transition metal oxides (TMO) or sulfides (TMS) appeared as potential competitors for the next generation of electrode materials in LIBs due to their large theoretical capacities (500–1000 mA h g^{-1}) and abundant reserves and low cost.[138–140] Taking this into account, the Wang group prepared yolk–shell Co$_3$O$_4$@CuO microspheres, which was followed by surface modification of carboxyl functionalized GQDs.[141] The results are shown in Fig. 8d; as an anode material in LIBs, NiO@Co$_3$O$_4$@GQDs provide a relatively large reversible capacity of about 1158 mA h g^{-1} after 250 cycles and a current density of 0.1 A g^{-1}, while the reversible capacity of NiO@Co$_3$O$_4$ is only about 1327 mA h g^{-1}. In addition, the GQDs wrapped on the outer surfaces of the Co$_3$O$_4$@CuO microspheres effectively maintain the durability of anodes, making the anode material GQDs@Co$_3$O$_4$@CuO have better cycle capacity and exhibit superior lithium storage performance, yielding a high initial specific capacity (816 mA h g^{-1}) and a high reversible charging capacity of 1054 mA g^{-1} after 200 cycles and 0.1 mA g^{-1} (Fig. 8d). On the other hand, transition metal
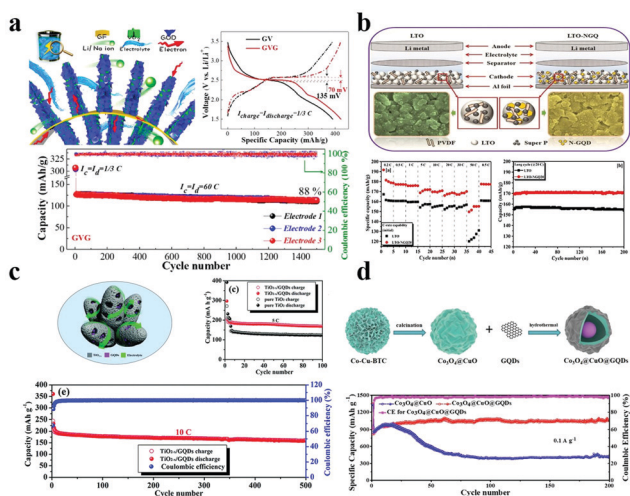
Fig. 8 Electrochemical characterization for batteries with GQDs. (a) The GVG electrode with GQDs in Li$^+$ and Na$^+$ batteries and the electrochemical performance. (Reproduced with permission from ref. 124, copyright 2015 American Chemical Society.) (b) The electrochemical performance of LTO-NGQ20 with rate capability from 0.2C to 50C and long cycling performance electrodes. (Reproduced with permission from ref. 129, copyright 2019 Elsevier B.V.) (c) The electrochemical reaction process of TiO$_{2-x}$/GQDs. (Reproduced with permission from ref. 137, copyright 2018 the Royal Society of Chemistry.) (d) The preparation of Co$_3$O$_4$@CuO@GQDs and the long-term cycling performance. (Reproduced with permission from ref. 141, copyright 2019 Elsevier B.V.)

disulfides have become the focus of research and application owing to their specific 2D layered feature, electronic structure, and unique physical and chemical properties.[142,143] Among them, molybdenum disulfide (MoS_2) exhibits excellent performance in energy storage and conversion. It is a pity that the practical application of a MoS_2 anode is hindered by its intrinsic pulverization, which in turn induces rapid capacity degradation and poor cycling performance. In order to overcome this obstacle, the Zhang group first reported a facile synthesis of GQD doped MoS_2 nanosheets *via* a solvothermal process.[116] The obtained GQD/MoS_2 material manifests remarkably improved electrochemical lithium storage performance compared to the original MoS_2, such as high reversible capacity (1099 mA h g^{-1} at 100 mA g^{-1}), good cycle stability, and excellent rate performance (660 mA h g^{-1} at 5000 mA g^{-1}). Silicon is well known as the most promising anode material for high-capacity lithium ion batteries.[144] To date, several methods have been successfully used for improving the electrochemical properties of silicon anodes.[145,146] However, the development of silicon particles is limited by their size and electrical conductivity. With this in mind, the Li group reported the use of GQDs in a silicon anode.[119] The effect of the coating layer on the diffusion of lithium ions between the silicon surface and the electrolyte will be reduced to a very low level. This work provides an easy method to design and prepare silicon-based anode materials for next-generation high performance lithium ion batteries.

4.4 Light-emitting diodes

Since graphene was discovered by Geim and Novoselov,[147] its high carrier mobility and linear dispersion band structure make it a promising candidate for optoelectrical applications. However, as bulk graphene does not have a band gap, it has limitations in further applications. Compared to bulk graphene, GQDs have quantum confinement and edge effects, so the band gap that changes carrier behaviour exists in GQDs and makes their applications in photodetection,[58,148] photovoltaics,[149,150] light-emitting diodes (LEDs)[151,152] and plasmonics[153,154] more versatile. Among these applications, LEDs have a bright future due to their energy saving, environmental protection and long cycling lives. The basic principle of GQD-based LED illumination is as follows: an external electric field excites carriers and then emits light after immediate recombination. In LEDs, GQDs can act as the electroluminescent phosphor,[155–157] dopant,[151] gap tuner[70] or color converter.[158] In the area of electroluminescent phosphors, Kim et al. fabricated highly-efficient LEDs based on octadecylamine (ODA) GQDs.[156] The amount of oxygen components in the ODA-GQDs was lower than that in pure GQDs due to nucleophilic substitution between the amine and the epoxy functional groups. The current efficiency of the ODA-GQD-based LEDs is 6.51 cd A^{-1} (Fig. 9a) and is the highest among the efficiencies reported for GQD-based LEDs.

In addition, a new luminescent material (GQD@ZIF-8) was synthesized by incorporating edge-sulfonated GQDs as active fluorescent species into a zeolitic imidazolate framework (ZIF-8) as a stabilizer and carrier.[157] In white LEDs, GQD@ZIF-8 was used as a novel yellow phosphor based on a blue-light LED chip
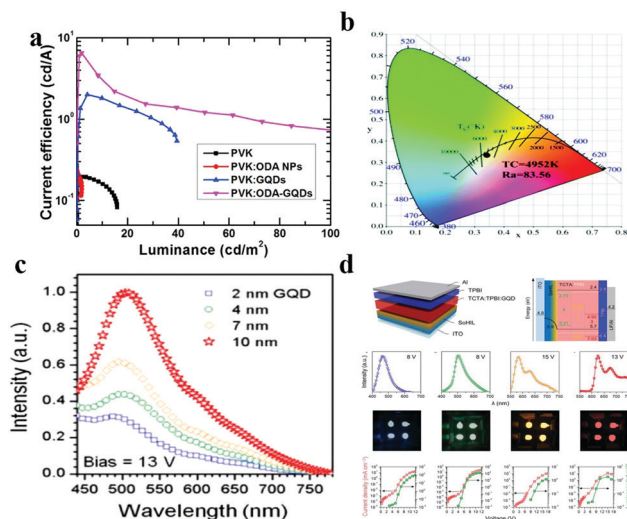

Fig. 9 GQDs for light-emitting diode applications. (a) Current efficiency–luminance for LEDs with PVK, PVK:ODA NPs, PVK:GQDs and PVK:ODA-GQDs. (Reproduced with permission from ref. 156, copyright 2017 Elsevier B.V.) (b) The CIE color coordinates, CRI values, and CCT values for white LED lamps fabricated by integrating a 450 nm blue chip with GQD@ZIF-8. (Reproduced with permission from ref. 157, copyright 2018 the Royal Society of Chemistry.) (c) Electroluminescence spectra of an OLED using GQDs as a light emitter at a bias of 13 V. (Reproduced with permission from ref. 151, copyright 2014 American Chemical Society.) (d) LED structure, energy levels, electroluminescence spectra, photographs of blue, green, orange and red LEDs using aniline derivative functionalized GQDs as band gap tuners. (Reproduced with permission from ref. 148, copyright 2014 Nature.)

with proximate CIE coordinates of (0.33, 0.33) of highly pure white light and a larger color-rendering index (Fig. 9b). In the field of dopants, Rhee et al. first reported the electroluminescence of GQDs and organic LEDs with GQDs, which exhibited white light emission with an external quantum efficiency of ∼0.1%.[151] They demonstrated OLEDs employing 4,4′-bis(carbazol-9-yl)biphenyl (CBP) as a host and a series of GQDs which have advantages such as appropriate energy-band structures and excellent organic solubility as dopants. As shown in Fig. 9c, with the increasing size of the GQDs, the electroluminescence (EL) intensity is also increased at a fixed bias. This is because the lower band-gaps of large size GQDs facilitate energy transfer from the host to the GQDs, which is the most important process for achieving bright electroluminescence. In addition, as the size of the GQDs increases from 2 nm to 10 nm, the Commission Internationale de l'Éclairage chromaticity diagram indicates that the EL color shifts from red to blue. When GQDs are used as a band gap tuner in the active layer, the problems of poor color purity and color tunability of the LEDs are perfectly solved. An aniline derivative is used by Rhee et al. to chemically functionalize GQDs, which causes GQDs to generate new extrinsic energy levels and very narrow linewidths of light, resulting in a red-shifted electroluminescence effect and improved color purity.[70] The maximum current efficiency of the LED is 3.47 cd A^{-1} and the external quantum efficiency is 1.28%, which is the highest value for carbon nanoparticle phosphor-based LEDs. Lau and his co-workers synthesized a GQD–agar composite, as a color converter, which works in color conversion materials in blue LEDs

This journal is © The Royal Society of Chemistry and the Chinese Chemical Society 2020

Mater. Chem. Front., 2020, 4, 421–436 | 431

to achieve white light emission (Fig. 9d). It also exhibits excellent optical stability and no observable luminescence quenching. The white LED has a luminous efficiency of 42.2 lm W^{-1}, and its light conversion efficiency (61.1%) for continuous operation over 100 h is very stable.

4.5 Other applications

GQDs, an advanced multifunctional material, have been introduced into the development of energy conversion devices due to their unique optical and photoelectric properties. GQD-based energy converters have the ability to convert heat, light, moisture, pressure and other forms of energy into electrical energy.

Taking advantage of the fact that GQD fillers can improve the charge capture effect at the material phase interface, the Bakar group established a nanogenerator that achieves a higher output voltage and produces a positive polarity output signal of 4.6 V wide and 48 ms wide.[159] The results show that the nanogenerator could successfully light up an LED when connected to an external circuit, and work steadily for up to 60 h (Fig. 10a). These superior properties are primarily dependent on the ability of GQDs to increase sensitivity to mechanical stimulations. In the Kim group, researchers applied GQDs on Ag nanowires to increase the sensitivity of external mechanical stimulation of the material.[160] As shown in Fig. 10b, GQDs significantly increase the output current of the as-prepared product. Normally, when the electronic skin is under a pressure of 10 N, the GQDs (G-Ag-NWs) can output a short-circuit current density of $\sim$10 mA cm^{-2}, which is 20 times that without GQDs. On the other hand, GQDs as an active material can produce a high-performance moisture-triggered nanogenerator. Ion concentration gradient induced electricity is a new form of energy conversion.[161,162] Here, GQDs act as an effective additive to improve the performance of moisture production and power generation. The Berry group established the first GQD-based electronic humidity sensor that produces approximately 60 nA at 0.4 V when the atmosphere changes from humid air to helium.[163] The results showed that due to the GQD additive, the tunnel barrier width can be reduced by 0.36 nm and the conductivity of the device can be increased by 43 times (Fig. 10c). The Qu group demonstrated a GQD-based electricity nanogenerator, in which electrochemical polarization treatment could generate a high voltage of up to 0.27 V under 70% change in relative humidity.[164] After optimizing the load resistance, the power density is 1.86 mW cm^{-2} (Fig. 10d). Therefore, by self-assembling GQDs onto polymer microfibers to form a permeable network, it is possible to construct a humidity and pressure sensor that operates by electronic tunnel modulation using the hygroscopic nature of the polymer. In 2017, the Pan group proposed a novel recipe to fabricate Bi$_2$Te$_3$/GQD hybrid nanosheets, in which GQDs can be uniformly embedded in a Bi$_2$Te$_3$ nanosheet matrix, revealing that GQDs may affect carrier transport behavior. Importantly, the thermoelectric performance of Bi$_2$Te$_3$/GQD hybrid nanostructures could be further enhanced by the optimization of the density and dispersion manner of GQDs in the Bi$_2$Te$_3$ matrix.[165] Recently, the entry of GQDs in the field of photocatalysis for solar energy harvesting and conversion attracted increasing attention. In 2017,
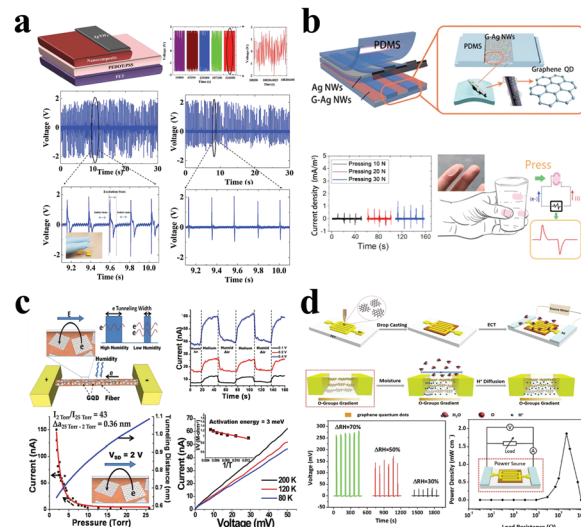
Fig. 10 GQDs for other energy conversion applications. (a) GQDs mixed with barium titanate for a nanogenerator device. (Reproduced with permission from ref. 159, copyright 2018 Elsevier B.V.) (b) Triboelectric electronic skin based on GQDs. (Reproduced with permission from ref. 160, copyright 2018 Elsevier B.V.) (c) The device with a GQD network and humidity/pressure sensors. (Reproduced with permission from ref. 163, copyright 2013 American Chemical Society.) (d) Moisture-triggered nanogenerator based on GQDs. (Reproduced with permission from ref. 164, copyright 2017 American Chemical Society.)

highly-ordered metal/GQD nanocomposites with fine structural control were fabricated by the Xiao group.[166] These (M/GQDs)$_n$ (M = Au, Ag, Pt) multilayer thin films exhibited highly-efficient and versatile catalytic performance under ambient conditions. Most importantly, the authors found that the catalytic performances of the (M/GQDs)$_n$ multilayer thin films can be optimized by tuning the assembly cycle and sequence, as well as by selecting different types of metal NPs. After that, some prominent photoelectrochemical works based on GQDs and nanoclusters have been reported.[167,168] These studies open new technical methods for high-efficiency solar energy harvesting and conversion.

5 Summary and prospects

GQDs have important applications in the field of energy storage and conversion due to their special structure and intrinsic properties. In recent years, the research on SCs/MSCs using simple GQDs as electrodes has become less and less. Instead, studies of pseudocapacitive SCs with GQDs as conductive agents have increased vigorously. This trend is in line with the pursuit of greater capacity. However, the doping and modification of GQDs results in a decrease in their conductivity. Doping some heteroatoms can make GQDs possess pseudocapacitive characteristics. Due to their unique optoelectronic properties, upconversion field luminescence properties and band gap tunability, the incorporation of GQDs into nanomaterials increases the ability of charge carrier extraction to improve solar cell efficiency. GQDs have a large specific surface area, high electron mobility and excellent UV absorption and the ability to convert

432 | *Mater. Chem. Front.*, 2020, **4**, 421–436

This journal is © The Royal Society of Chemistry and the Chinese Chemical Society 2020

into visible light. Therefore, GQDs are widely used as sensitizers, electron/hole transport layers or active layer additives for photosensitive devices. In Li^+/Na^+ batteries, GQDs can effectively alleviate volume expansion, increase the ion diffusion rate and electron transfer, improve the interfacial electrical double layer and enhance electrochemical performance. Since bulk graphene does not have a band gap, it shows great limitations in further applications. Compared with bulk graphene, GQDs have quantum confinement and edge effects, so band gaps which modify carrier behavior exist in GQDs and enlarge their applications in LEDs. GQD-based energy converters can collect heat and convert it into electricity or convert it into energy such as electricity through light, moisture, pressure and other forms of energy.

Although GQDs and their applications have made great progress in recent years, there are still many problems to be solved. In general, the first problem is that there is no clear definition of the actual size of GQDs, which has a great impact on the subsequent research of GQDs. For small-scale research, tiny differences will be amplified, even if the difference is only a few nanometers. The lack of size definition results in a very broad size range of graphene quantum dots. This problem also makes the physical and chemical properties of graphene quantum dots unclear. The industrial production and green synthesis of GQDs is another problem that needs to be addressed urgently. The inability to industrialize production has made it difficult to reduce the manufacturing cost of GQDs, which seriously affects the practical application of GQDs. Fortunately, the production of GQDs by green chemistry has received more attention in recent years. The synthesis of GQDs is progressing towards low pollution, low toxicity and low energy consumption, and there is still room for further improvement in these methods. In particular, there is still great room for development in the combination of green chemical synthesis and low-cost industrial production. We believe that GQD-based research will show great potential in these directions.

Conflicts of interest

There are no conflicts to declare.

Acknowledgements

Notes and references

1 Y. Zhu, S. Murali, W. Cai, X. Li, J. W. Suk, J. R. Potts and R. S. Ruoff, *Adv. Mater.*, 2010, **22**, 3906–3924.

2 M. J. Sweetman, S. M. Hickey, D. A. Brooks, J. D. Hayball and S. E. Plush, *Adv. Funct. Mater.*, 2019, **29**, 1808740.

3 X. Wang, G. Sun, N. Li and P. Chen, *Chem. Soc. Rev.*, 2016, **45**, 2239–2262.

4 X. T. Zheng, A. Ananthanarayanan, K. Q. Luo and P. Chen, *Small*, 2015, **11**, 1620–1636.

5 L. Li, G. Wu, G. Yang, J. Peng, J. Zhao and J.-J. Zhu, *Nanoscale*, 2013, **5**, 4015–4039.

6 D. Pan, J. Zhang, Z. Li and M. Wu, *Adv. Mater.*, 2010, **22**, 734–738.

7 X. Zhou, Y. Zhang, C. Wang, X. Wu, Y. Yang, B. Zheng, H. Wu, S. Guo and J. Zhang, *ACS Nano*, 2012, **6**, 6592–6599.

8 H. Sun, L. Wu, W. Wei and X. Qu, *Mater. Today*, 2013, **16**, 433–442.

9 X. Hai, J. Feng, X. Chen and J. Wang, *J. Mater. Chem. B*, 2018, **6**, 3219–3234.

10 N. Fuyuno, D. Kozawa, Y. Miyauchi, S. Mouri, R. Kitaura, H. Shinohara, T. Yasuda, N. Komatsu and K. Matsuda, *Adv. Opt. Mater.*, 2014, **2**, 983–989.

11 K. Li, W. Liu, Y. Ni, D. Li, D. Lin, Z. Su and G. Wei, *J. Mater. Chem. B*, 2017, **5**, 4811–4826.

12 S. Kim, D. H. Shin, C. O. Kim, S. S. Kang, S. S. Joo, S.-H. Choi, S. W. Hwang and C. Sone, *Appl. Phys. Lett.*, 2013, **102**, 053108.

13 S. Kim, D. H. Shin, C. O. Kim, S. S. Kang, J. M. Kim, S.-H. Choi, L.-H. Jin, Y.-H. Cho, S. W. Hwang and C. Sone, *Appl. Phys. Lett.*, 2012, **101**, 163103.

14 J. Peng, W. Gao, B. K. Gupta, Z. Liu, R. Romero-Aburto, L. Ge, L. Song, L. B. Alemany, X. Zhan, G. Gao, S. A. Vithayathil, B. A. Kaipparettu, A. A. Marti, T. Hayashi, J.-J. Zhu and P. M. Ajayan, *Nano Lett.*, 2012, **12**, 844–849.

15 Y. Yan, J. Gong, J. Chen, Z. Zeng, W. Huang, K. Pu, J. Liu and P. Chen, *Adv. Mater.*, 2019, **31**, 1808283.

16 P. Zheng and N. Wu, *Chem. – Asian J.*, 2017, **12**, 2343–2353.

17 M. Li, T. Chen, J. J. Gooding and J. Liu, *ACS Sens.*, 2019, **4**, 1732–1748.

18 X. Li, J. Yu, S. Wageh, A. A. Al-Ghamdi and J. Xie, *Small*, 2016, **12**, 6640–6696.

19 Z. Zeng, S. Chen, T. T. Y. Tan and F.-X. Xiao, *Catal. Today*, 2018, **315**, 171–183.

20 E. Haque, J. Kim, V. Malgras, K. R. Reddy, A. C. Ward, J. You, Y. Bando, M. S. A. Hossain and Y. Yamauchi, *Small Methods*, 2018, **2**, 1800050.

21 X. Li, M. Rui, J. Song, Z. Shen and H. Zeng, *Adv. Funct. Mater.*, 2015, **25**, 4929–4947.

22 S. Zhu, Q. Meng, L. Wang, J. Zhang, Y. Song, H. Jin, K. Zhang, H. Sun, H. Wang and B. Yang, *Angew. Chem., Int. Ed.*, 2013, **125**, 4045–4049.

23 Y. Xu, X.-H. Jia, X.-B. Yin, X.-W. He and Y.-K. Zhang, *Anal. Chem.*, 2014, **86**, 12122–12129.

24 Q. Liu, B. Guo, Z. Rao, B. Zhang and J. R. Gong, *Nano Lett.*, 2013, **13**, 2436–2441.

25 A. Ananthanarayanan, X. Wang, P. Routh, B. Sana, S. Lim, D.-H. Kim, K.-H. Lim, J. Li and P. Chen, *Adv. Funct. Mater.*, 2014, **24**, 3021–3026.

26 D. B. Shinde and V. K. Pillai, *Chem. – Eur. J.*, 2012, **18**, 12522–12528.

27 L. Nilewski, K. Mendoza, A. S. Jalilov, V. Berka, G. Wu, W. K. A. Sikkema, A. Metzger, R. Ye, R. Zhang, D. X. Luong, T. Wang, E. McHugh, P. J. Derry, E. L. Samuel, T. A. Kent,

This journal is © The Royal Society of Chemistry and the Chinese Chemical Society 2020

Mater. Chem. Front., 2020, **4**, 421–436 | **433**

A.-L. Tsai and J. M. Tour, *ACS Appl. Mater. Interfaces*, 2019, **11**, 16815–16821.

28 J. Wen, M. Li, J. Xiao, C. Liu, Z. Li, Y. Xie, P. Ning, H. Cao and Y. Zhang, *Mater. Today. Commun.*, 2016, **8**, 127–133.

29 L. Lu, Y. Zhu, C. Shi and Y. T. Pei, *Carbon*, 2016, **109**, 373–383.

30 V. Amendola and M. Meneghetti, *Phys. Chem. Chem. Phys.*, 2009, **11**, 3805–3821.

31 G. W. Yang, *Prog. Mater. Sci.*, 2007, **52**, 648–698.

32 J. Pal, M. Ganguly, C. Mondal, Y. Negishi and T. Pal, *Nanoscale*, 2015, **7**, 708–719.

33 S. R. M. Santiago, T. N. Lin, C. T. Yuan, J. L. Shen, H. Y. Huang and C. A. J. Lin, *Phys. Chem. Chem. Phys.*, 2016, **18**, 22599–22605.

34 S.-J. Jeon, T.-W. Kang, J.-M. Ju, M.-J. Kim, J. H. Park, F. Raza, J. Han, H.-R. Lee and J.-H. Kim, *Adv. Funct. Mater.*, 2016, **26**, 8211–8219.

35 J. Zhu, Y. Tang, G. Wang, J. Mao, Z. Liu, T. Sun, M. Wang, D. Chen, Y. Yang, J. Li, Y. Deng and S. Yang, *ACS Appl. Mater. Interfaces*, 2017, **9**, 14470–14477.

36 Y. Dong, J. Shao, C. Chen, H. Li, R. Wang, Y. Chi, X. Lin and G. Chen, *Carbon*, 2012, **50**, 4738–4743.

37 D. Qu, M. Zheng, P. Du, Y. Zhou, L. Zhang, D. Li, H. Tan, Z. Zhao, Z. Xie and Z. Sun, *Nanoscale*, 2013, **5**, 12272–12277.

38 R. Zhang, J. R. Adsetts, Y. Nie, X. Sun and Z. Ding, *Carbon*, 2018, **129**, 45–53.

39 H. Jin, H. Huang, Y. He, X. Feng, S. Wang, L. Dai and J. Wang, *J. Am. Chem. Soc.*, 2015, **137**, 7588–7591.

40 A. Suryawanshi, M. Biswal, D. Mhamane, R. Gokhale, S. Patil, D. Guin and S. Ogale, *Nanoscale*, 2014, **6**, 11664–11670.

41 Z. Wang, J. Yu, X. Zhang, N. Li, B. Liu, Y. Li, Y. Wang, W. Wang, Y. Li, L. Zhang, S. Dissanayake, S. L. Suib and L. Sun, *ACS Appl. Mater. Interfaces*, 2016, **8**, 1434–1439.

42 R. Riaz, M. Ali, I. A. Sahito, A. A. Arbab, T. Maiyalagan, A. S. Anjum, M. J. Ko and S. H. Jeong, *Appl. Surf. Sci.*, 2019, **480**, 1035–1046.

43 W.-S. Kuo, Y.-T. Shao, K.-S. Huang, T.-M. Chou and C.-H. Yang, *ACS Appl. Mater. Interfaces*, 2018, **10**, 14438–14446.

44 F. Zuo, C. Zhang, H. Zhang, X. Tan, S. Chen and R. Yuan, *Electrochim. Acta*, 2019, **294**, 76–83.

45 Y. Fu, G. Gao and J. Zhi, *J. Mater. Chem. B*, 2019, **7**, 1494–1502.

46 Y. Guo, F. Cao and Y. Li, *Sens. Actuators, B*, 2018, **255**, 1105–1111.

47 D. Shen, W. Zhang, F. Xie, Y. Li, A. Abate and M. Wei, *J. Power Sources*, 2018, **402**, 320–326.

48 Z. Li, L. Cao, P. Qin, X. Liu, Z. Chen, L. Wang, D. Pan and M. Wu, *Carbon*, 2018, **139**, 67–75.

49 M. T. Hasan, R. Gonzalez-Rodriguez, C. Ryan, K. Pota, K. Green, J. L. Coffer and A. V. Naumov, *Nano Res.*, 2019, **12**, 1041–1047.

50 S. Yang, J. Sun, P. He, X. Deng, Z. Wang, C. Hu, G. Ding and X. Xie, *Chem. Mater.*, 2015, **27**, 2004–2011.

51 Y. Zhang, J. Zhao, H. Sun, Z. Zhu, J. Zhang and Q. Liu, *Sens. Actuators, B*, 2018, **266**, 364–374.

52 L. S. Walekar, M. Zheng, L. Zheng and M. Long, *Microchim. Acta*, 2019, **186**, 278.

53 D. Wei, Y. Liu, Y. Wang, H. Zhang, L. Huang and G. Yu, *Nano Lett.*, 2009, **9**, 1752–1758.

54 C.-P. Han, C.-J. Chen, C.-C. Hsu, A. Jena, H. Chang, N.-C. Yeh, S.-F. Hu and R.-S. Liu, *Catal. Today*, 2019, **335**, 395–401.

55 H. Safardoust-Hojaghan and M. Salavati-Niasari, *J. Cleaner Prod.*, 2017, **148**, 31–36.

56 J. Moon, J. An, U. Sim, S.-P. Cho, J. H. Kang, C. Chung, J.-H. Seo, J. Lee, K. T. Nam and B. H. Hong, *Adv. Mater.*, 2014, **26**, 3501–3505.

57 Y. Li, Y. Zhao, H. Cheng, Y. Hu, G. Shi, L. Dai and L. Qu, *J. Am. Chem. Soc.*, 2012, **134**, 15–18.

58 L. Tang, R. Ji, X. Li, G. Bai, C. P. Liu, J. Hao, J. Lin, H. Jiang, K. S. Teng, Z. Yang and S. P. Lau, *ACS Nano*, 2014, **8**, 6312–6320.

59 T. V. Tam, S. G. Kang, M. H. Kim, S. G. Lee, S. H. Hur, J. S. Chung and W. M. Choi, *Adv. Energy Mater.*, 2019, **9**, 1900945.

60 H. Wang, R. Revia, K. Wang, R. J. Kant, Q. Mu, Z. Gai, K. Hong and M. Zhang, *Adv. Mater.*, 2017, **29**, 1605416.

61 T. Van Tam, S. G. Kang, K. F. Babu, E.-S. Oh, S. G. Lee and W. M. Choi, *J. Mater. Chem. A*, 2017, **5**, 10537–10543.

62 M. T. Hasan, R. Gonzalez-Rodriguez, C. Ryan, N. Faerber, J. L. Coffer and A. V. Naumov, *Adv. Funct. Mater.*, 2018, **28**, 1804337.

63 S. Kundu, R. M. Yadav, T. N. Narayanan, M. V. Shelke, R. Vajtai, P. M. Ajayan and V. K. Pillai, *Nanoscale*, 2015, **7**, 11515–11519.

64 S. Kundu, P. Sarojinijeeva, R. Karthick, G. Anantharaj, G. Saritha, R. Bera, S. Anandan, A. Patra, P. Ragupathy, M. Selvaraj, D. Jeyakumar and K. V. Pillai, *Electrochim. Acta*, 2017, **242**, 337–343.

65 H. Sun, A. Zhao, N. Gao, K. Li, J. Ren and X. Qu, *Angew. Chem., Int. Ed.*, 2015, **54**, 7176–7180.

66 A. Shomali, H. Valizadeh, A. Banan and R. Mohammad-Rezaei, *RSC Adv.*, 2015, **5**, 88202–88208.

67 K. Li, J. Chen, Y. Yan, Y. Min, H. Li, F. Xi, J. Liu and P. Chen, *Carbon*, 2018, **136**, 224–233.

68 H. Tetsuka, R. Asahi, A. Nagoya, K. Okamoto, I. Tajima, R. Ohta and A. Okamoto, *Adv. Mater.*, 2012, **24**, 5333–5338.

69 B.-P. Qi, H. Hu, L. Bao, Z.-L. Zhang, B. Tang, Y. Peng, B.-S. Wang and D.-W. Pang, *Nanoscale*, 2015, **7**, 5969–5973.

70 W. Kwon, Y.-H. Kim, J.-H. Kim, T. Lee, S. Do, Y. Park, M. S. Jeong, T.-W. Lee and S.-W. Rhee, *Sci. Rep.*, 2016, **6**, 24205.

71 H. Tetsuka, A. Nagoya, T. Fukusumi and T. Matsui, *Adv. Mater.*, 2016, **28**, 4632–4638.

72 Y. Yan, J. Chen, N. Li, J. Tian, K. Li, J. Jiang, J. Liu, Q. Tian and P. Chen, *ACS Nano*, 2018, **12**, 3523–3532.

73 W.-W. Liu, Y.-Q. Feng, X.-B. Yan, J.-T. Chen and Q.-J. Xue, *Adv. Funct. Mater.*, 2013, **23**, 4111–4122.

74 K. Lee, H. Lee, Y. Shin, Y. Yoon, D. Kim and H. Lee, *Nano Energy*, 2016, **26**, 746–754.

75 Z. Li, X. Liu, L. Wang, F. Bu, J. Wei, D. Pan and M. Wu, *Small*, 2018, **14**, 1801498.

76 W. Liu, X. Yan, J. Chen, Y. Feng and Q. Xue, *Nanoscale*, 2013, **5**, 6053–6062.

77 Y. Qing, Y. Jiang, H. Lin, L. Wang, A. Liu, Y. Cao, R. Sheng, Y. Guo, C. Fan, S. Zhang, D. Jia and Z. Fan, *J. Mater. Chem. A*, 2019, **7**, 6021–6027.

78 X. Yin, C. Zhi, W. Sun, L.-P. Lv and Y. Wang, *J. Mater. Chem. A*, 2019, **7**, 7800–7814.

79 B. Shen, J. Lang, R. Guo, X. Zhang and X. Yan, *ACS Appl. Mater. Interfaces*, 2015, **7**, 25378–25389.

80 S. Zhang, J. Zhu, Y. Qing, L. Wang, J. Zhao, J. Li, W. Tian, D. Jia and Z. Fan, *Adv. Funct. Mater.*, 2018, **28**, 1805898.

81 Z. Li, P. Qin, L. Wang, C. Yang, Y. Li, Z. Chen, D. Pan and M. Wu, *Electrochim. Acta*, 2016, **208**, 260–266.

82 A. B. Ganganboina, A. D. Chowdhury and R.-a. Doong, *Electrochim. Acta*, 2017, **245**, 912–923.

83 Y. Huang, T. Shi, Y. Zhong, S. Cheng, S. Jiang, C. Chen, G. Liao and Z. Tang, *Electrochim. Acta*, 2018, **269**, 45–54.

84 Q. Chen, Y. Hu, C. Hu, H. Cheng, Z. Zhang, H. Shao and L. Qu, *Phys. Chem. Chem. Phys.*, 2014, **16**, 19307–19313.

85 S. H. Shin, D. H. Shin and S.-H. Choi, *ACS Sustainable Chem. Eng.*, 2019, **7**, 13178–13185.

86 L. Najafi, B. Taheri, B. Martín-García, S. Bellani, D. Di Girolamo, A. Agresti, R. Oropesa-Nuñez, S. Pescetelli, L. Vesce, E. Calabrò, M. Prato, A. E. Del Rio Castillo, A. Di Carlo and F. Bonaccorso, *ACS Nano*, 2018, **12**, 10736–10754.

87 K. D. Lee, M. J. Park, D.-Y. Kim, S. M. Kim, B. Kang, S. Kim, H. Kim, H.-S. Lee, Y. Kang, S. S. Yoon, B. H. Hong and D. Kim, *ACS Appl. Mater. Interfaces*, 2015, **7**, 19043–19049.

88 D. Torres, D. Sebastián, M. J. Lázaro, J. L. Pinilla, I. Suelves, A. S. Aricò and V. Baglio, *Electrochim. Acta*, 2019, **306**, 396–406.

89 T. Liu, K. Yu, L. Gao, H. Chen, N. Wang, L. Hao, T. Li, H. He and Z. Guo, *J. Mater. Chem. A*, 2017, **5**, 17848–17855.

90 H. Sung, N. Ahn, M. S. Jang, J.-K. Lee, H. Yoon, N.-G. Park and M. Choi, *Adv. Energy Mater.*, 2016, **6**, 1501873.

91 Z.-K. Wang, X. Gong, M. Li, Y. Hu, J.-M. Wang, H. Ma and L.-S. Liao, *ACS Nano*, 2016, **10**, 5479–5489.

92 G. S. Han, Y. H. Song, Y. U. Jin, J.-W. Lee, N.-G. Park, B. K. Kang, J.-K. Lee, I. S. Cho, D. H. Yoon and H. S. Jung, *ACS Appl. Mater. Interfaces*, 2015, **7**, 23521–23526.

93 J. Ryu, E. Lee, S. Lee and J. Jang, *Chem. Commun.*, 2014, **50**, 15616–15618.

94 J. Ryu, J. W. Lee, H. Yu, J. Yun, K. Lee, J. Lee, D. Hwang, J. Kang, S. K. Kim and J. Jang, *J. Mater. Chem. A*, 2017, **5**, 16834–16842.

95 T. Mahmoudi, Y. Wang and Y.-B. Hahn, *ACS Energy Lett.*, 2019, **4**, 235–241.

96 Y. Wang, T. Mahmoudi, W.-Y. Rho, H.-Y. Yang, S. Seo, K. S. Bhat, R. Ahmad and Y.-B. Hahn, *Nano Energy*, 2017, **40**, 408–417.

97 H. Bian, Q. Wang, S. Yang, C. Yan, H. Wang, L. Liang, Z. Jin, G. Wang and S. Liu, *J. Mater. Chem. A*, 2019, **7**, 5740–5747.

98 M. Tai, X. Zhao, H. Wei, G. Wang, F. Hao, X. Li, X. Yin, Y. Zhou, J. Han, Y. Wei, K. Jiang and H. Lin, *ACS Appl. Mater. Interfaces*, 2018, **10**, 26206–26212.

99 G. Xing, B. Wu, S. Chen, J. Chua, N. Yantara, S. Mhaisalkar, N. Mathews and T. C. Sum, *Small*, 2015, **11**, 3606–3613.

100 W. Tress, N. Marinova, T. Moehl, S. M. Zakeeruddin, M. K. Nazeeruddin and M. Grätzel, *Energy Environ. Sci.*, 2015, **8**, 995–1004.

101 H. Tan, A. Jain, O. Voznyy, X. Lan, F. P. García de Arquer, J. Z. Fan, R. Quintero-Bermudez, M. Yuan, B. Zhang, Y. Zhao, F. Fan, P. Li, L. N. Quan, Y. Zhao, Z.-H. Lu, Z. Yang, S. Hoogland and E. H. Sargent, *Science*, 2017, **355**, 722–726.

102 Y. Zhou, S. Yang, X. Yin, J. Han, M. Tai, X. Zhao, H. Chen, Y. Gu, N. Wang and H. Lin, *J. Mater. Chem. A*, 2019, **7**, 1878–1888.

103 W. Ke, G. Fang, Q. Liu, L. Xiong, P. Qin, H. Tao, J. Wang, H. Lei, B. Li, J. Wan, G. Yang and Y. Yan, *J. Am. Chem. Soc.*, 2015, **137**, 6730–6733.

104 X. Liu, K.-W. Tsai, Z. Zhu, Y. Sun, C.-C. Chueh and A. K.-Y. Jen, *Adv. Mater. Interfaces*, 2016, **3**, 1600122.

105 W. Ke, D. Zhao, C. Xiao, C. Wang, A. J. Cimaroli, C. R. Grice, M. Yang, Z. Li, C.-S. Jiang, M. Al-Jassim, K. Zhu, M. G. Kanatzidis, G. Fang and Y. Yan, *J. Mater. Chem. A*, 2016, **4**, 14276–14283.

106 E. H. Anaraki, A. Kermanpur, L. Steier, K. Domanski, T. Matsui, W. Tress, M. Saliba, A. Abate, M. Grätzel, A. Hagfeldt and J.-P. Correa-Baena, *Energy Environ. Sci.*, 2016, **9**, 3128–3134.

107 J. P. Correa Baena, L. Steier, W. Tress, M. Saliba, S. Neutzner, T. Matsui, F. Giordano, T. J. Jacobsson, A. R. Srimath Kandada, S. M. Zakeeruddin, A. Petrozza, A. Abate, M. K. Nazeeruddin, M. Grätzel and A. Hagfeldt, *Energy Environ. Sci.*, 2015, **8**, 2928–2934.

108 J. Xie, K. Huang, X. Yu, Z. Yang, K. Xiao, Y. Qiang, X. Zhu, L. Xu, P. Wang, C. Cui and D. Yang, *ACS Nano*, 2017, **11**, 9176–9182.

109 J. H. Kim, C.-C. Chueh, S. T. Williams and A. K. Y. Jen, *Nanoscale*, 2015, **7**, 17343–17349.

110 J. Xie, X. Yu, X. Sun, J. Huang, Y. Zhang, M. Lei, K. Huang, D. Xu, Z. Tang, C. Cui and D. Yang, *Nano Energy*, 2016, **28**, 330–337.

111 Z. Bin, J. Li, L. Wang and L. Duan, *Energy Environ. Sci.*, 2016, **9**, 3424–3428.

112 Z. Yang, J. Xie, V. Arivazhagan, K. Xiao, Y. Qiang, K. Huang, M. Hu, C. Cui, X. Yu and D. Yang, *Nano Energy*, 2017, **40**, 345–351.

113 M.-L. Tsai, W.-C. Tu, L. Tang, T.-C. Wei, W.-R. Wei, S. P. Lau, L.-J. Chen and J.-H. He, *Nano Lett.*, 2016, **16**, 309–313.

114 M.-L. Tsai, W.-R. Wei, L. Tang, H.-C. Chang, S.-H. Tai, P.-K. Yang, S. P. Lau, L.-J. Chen and J.-H. He, *ACS Nano*, 2016, **10**, 815–821.

115 M.-L. Tsai, D.-S. Tsai, L. Tang, L.-J. Chen, S. P. Lau and J.-H. He, *ACS Nano*, 2017, **11**, 4564–4570.

116 J. Guo, H. Zhu, Y. Sun, L. Tang and X. Zhang, *J. Mater. Chem. A*, 2016, **4**, 4783–4789.

117 Y.-M. Chen, S.-T. Hsu, Y.-H. Tseng, T.-F. Yeh, S.-S. Hou, J.-S. Jan, Y.-L. Lee and H. Teng, *Small*, 2018, **14**, 1703571.

118 J. Park, J. Moon, C. Kim, J. H. Kang, E. Lim, J. Park, K. J. Lee, S.-H. Yu, J.-H. Seo, J. Lee, J. Heo, N. Tanaka, S.-P. Cho, J. Pyun, J. Cabana, B. H. Hong and Y.-E. Sung, *NPG Asia Mater.*, 2016, **8**, e272.

119 K. Lijuan, Y. Yongqiang, L. Ruiyi and L. Zaijun, *Electrochim. Acta*, 2016, **198**, 144–155.

120 Y. Ji, J. Hu, J. Biskupek, U. Kaiser, Y.-F. Song and C. Streb, *Chem. – Eur. J.*, 2017, **23**, 16637–16643.

This journal is © The Royal Society of Chemistry and the Chinese Chemical Society 2020

Mater. Chem. Front., 2020, **4**, 421–436 | **435**

121 C. Zhu, D. Chao, J. Sun, I. M. Bacho, Z. Fan, C. F. Ng, X. Xia, H. Huang, H. Zhang, Z. X. Shen, G. Ding and H. J. Fan, *Adv. Mater. Interfaces*, 2015, **2**, 1400499.

122 J. Liu, H. Xia, D. Xue and L. Lu, *J. Am. Chem. Soc.*, 2009, **131**, 12086–12087.

123 D. Chao, X. Xia, J. Liu, Z. Fan, C. F. Ng, J. Lin, H. Zhang, Z. X. Shen and H. J. Fan, *Adv. Mater.*, 2014, **26**, 5794–5800.

124 D. Chao, C. Zhu, X. Xia, J. Liu, X. Zhang, J. Wang, P. Liang, J. Lin, H. Zhang, Z. X. Shen and H. J. Fan, *Nano Lett.*, 2015, **15**, 565–573.

125 J. M. Tarascon and M. Armand, *Nature*, 2001, **414**, 359–367.

126 A. S. Aricò, P. Bruce, B. Scrosati, J.-M. Tarascon and W. van Schalkwijk, *Nat. Mater.*, 2005, **4**, 366–377.

127 K. Kang, Y. S. Meng, J. Bréger, C. P. Grey and G. Ceder, *Science*, 2006, **311**, 977–980.

128 H.-G. Jung, M. W. Jang, J. Hassoun, Y.-K. Sun and B. Scrosati, *Nat. Commun.*, 2011, **2**, 516.

129 F. Khan, M. Oh and J. H. Kim, *Chem. Eng. J.*, 2019, **369**, 1024–1033.

130 J.-K. Sun and Q. Xu, *Energy Environ. Sci.*, 2014, **7**, 2071–2100.

131 S. J. Yang, T. Kim, J. H. Im, Y. S. Kim, K. Lee, H. Jung and C. R. Park, *Chem. Mater.*, 2012, **24**, 464–470.

132 J. Hu, H. Wang, Q. Gao and H. Guo, *Carbon*, 2010, **48**, 3599–3606.

133 J. Li, Y. Chen, Y. Tang, S. Li, H. Dong, K. Li, M. Han, Y.-Q. Lan, J. Bao and Z. Dai, *J. Mater. Chem. A*, 2014, **2**, 6316–6319.

134 H. Yu, W. Zhu, H. Zhou, J. Liu, Z. Yang, X. Hu and A. Yuan, *RSC Adv.*, 2019, **9**, 9577–9583.

135 B. Qiu, M. Xing and J. Zhang, *J. Am. Chem. Soc.*, 2014, **136**, 5852–5855.

136 Y. Zhang, C. W. Foster, C. E. Banks, L. Shao, H. Hou, G. Zou, J. Chen, Z. Huang and X. Ji, *Adv. Mater.*, 2016, **28**, 9391–9399.

137 W. Zhang, T. Xu, Z. Liu, N.-L. Wu and M. Wei, *Chem. Commun.*, 2018, **54**, 1413–1416.

138 D. Sun, Y. Tang, D. Ye, J. Yan, H. Zhou and H. Wang, *ACS Appl. Mater. Interfaces*, 2017, **9**, 5254–5262.

139 L. Qi, Y. Xin, Z. Zuo, C. Yang, K. Wu, B. Wu and H. Zhou, *ACS Appl. Mater. Interfaces*, 2016, **8**, 17245–17252.

140 H. Wang, J. Wang, D. Cao, H. Gu, B. Li, X. Lu, X. Han, A. L. Rogach and C. Niu, *J. Mater. Chem. A*, 2017, **5**, 6817–6824.

141 M. Wu, H. Chen, L.-P. Lv and Y. Wang, *Chem. Eng. J.*, 2019, **373**, 985–994.

142 R. Lv, J. A. Robinson, R. E. Schaak, D. Sun, Y. Sun, T. E. Mallouk and M. Terrones, *Acc. Chem. Res.*, 2015, **48**, 56–64.

143 H. Wang, H. Yuan, S. Sae Hong, Y. Li and Y. Cui, *Chem. Soc. Rev.*, 2015, **44**, 2664–2680.

144 I. Kovalenko, B. Zdyrko, A. Magasinski, B. Hertzberg, Z. Milicev, R. Burtovyy, I. Luzinov and G. Yushin, *Science*, 2011, **334**, 75–79.

145 M. Heurlin, M. H. Magnusson, D. Lindgren, M. Ek, L. R. Wallenberg, K. Deppert and L. Samuelson, *Nature*, 2012, **492**, 90.

146 S. Kawakami, H. Kaidou, Y. Akita, H. Munakata and K. Kanamura, *Electrochemistry*, 2015, **83**, 445–451.

147 K. S. Novoselov, A. K. Geim, S. V. Morozov, D. Jiang, Y. Zhang, S. V. Dubonos, I. V. Grigorieva and A. A. Firsov, *Science*, 2004, **306**, 666.

148 C. O. Kim, S. W. Hwang, S. Kim, D. H. Shin, S. S. Kang, J. M. Kim, C. W. Jang, J. H. Kim, K. W. Lee, S.-H. Choi and E. Hwang, *Sci. Rep.*, 2014, **4**, 5603.

149 K. J. Williams, C. A. Nelson, X. Yan, L.-S. Li and X. Zhu, *ACS Nano*, 2013, **7**, 1388–1394.

150 V. Gupta, N. Chaudhary, R. Srivastava, G. D. Sharma, R. Bhardwaj and S. Chand, *J. Am. Chem. Soc.*, 2011, **133**, 9960–9963.

151 W. Kwon, Y.-H. Kim, C.-L. Lee, M. Lee, H. C. Choi, T.-W. Lee and S.-W. Rhee, *Nano Lett.*, 2014, **14**, 1306–1311.

152 S. H. Song, M.-H. Jang, J. Chung, S. H. Jin, B. H. Kim, S.-H. Hur, S. Yoo, Y.-H. Cho and S. Jeon, *Adv. Opt. Mater.*, 2014, **2**, 1016–1023.

153 P. Alonso-González, A. Y. Nikitin, F. Golmar, A. Centeno, A. Pesquera, S. Vélez, J. Chen, G. Navickaite, F. Koppens, A. Zurutuza, F. Casanova, L. E. Hueso and R. Hillenbrand, *Science*, 2014, **344**, 1369.

154 H. Yan, X. Li, B. Chandra, G. Tulevski, Y. Wu, M. Freitag, W. Zhu, P. Avouris and F. Xia, *Nat. Nanotechnol.*, 2012, **7**, 330.

155 R. Sekiya, Y. Uemura, H. Murakami and T. Haino, *Angew. Chem., Int. Ed.*, 2014, **53**, 5619–5623.

156 D. H. Kim and T. W. Kim, *Nano Energy*, 2017, **32**, 441–447.

157 D. Pan, L. Wang, Z. Li, B. Geng, C. Zhang, J. Zhan, L. Yin and L. Wang, *New J. Chem.*, 2018, **42**, 5083–5089.

158 C. M. Luk, L. B. Tang, W. F. Zhang, S. F. Yu, K. S. Teng and S. P. Lau, *J. Mater. Chem.*, 2012, **22**, 22378–22381.

159 E. A. Bakar, M. A. Mohamed, P. C. Ooi, M. F. M. R. Wee, C. F. Dee and B. Y. Majlis, *Org. Electron.*, 2018, **61**, 289–295.

160 Z. Xu, C. Wu, F. Li, W. Chen, T. Guo and T. W. Kim, *Nano Energy*, 2018, **49**, 274–282.

161 Y. Zhao, R.-j. Tong, M.-Q. Chen and F. Xia, *Sens. Actuators, B*, 2019, **284**, 96–102.

162 P. Qi, T. Zhang, J. Shao, B. Yang, T. Fei and R. Wang, *Sens. Actuators, A*, 2019, **287**, 93–101.

163 T. S. Sreeprasad, A. A. Rodriguez, J. Colston, A. Graham, E. Shishkin, V. Pallem and V. Berry, *Nano Lett.*, 2013, **13**, 1757–1763.

164 Y. Huang, H. Cheng, G. Shi and L. Qu, *ACS Appl. Mater. Interfaces*, 2017, **9**, 38170–38175.

165 S. Li, T. Fan, X. Liu, F. Liu, H. Meng, Y. Liu and F. Pan, *ACS Appl. Mater. Interfaces*, 2017, **9**, 3677–3685.

166 Z. Zeng, F.-X. Xiao, H. Phan, S. Chen, Z. Yu, R. Wang, T.-Q. Nguyen and T. T. Yang Tan, *J. Mater. Chem. A*, 2018, **6**, 1700–1713.

167 Z. Zeng, Y.-B. Li, S. Chen, P. Chen and F.-X. Xiao, *J. Mater. Chem. A*, 2018, **6**, 11154–11162.

168 Z. Zeng, T. Li, Y.-B. Li, X.-C. Dai, M.-H. Huang, Y. He, G. Xiao and F.-X. Xiao, *J. Mater. Chem. A*, 2018, **6**, 24686–24692.

This journal is © The Royal Society of Chemistry and the Chinese Chemical Society 2020